Spatially Varying Spectral Filtering of Signals on the Unit Sphere

Zubair Khalid, *Student Member, IEEE*, Parastoo Sadeghi, *Senior Member, IEEE*, Rodney A. Kennedy, *Fellow, IEEE*, and Salman Durrani, *Senior Member, IEEE*

***Abstract*—This paper presents a general framework for spatially-varying spectral filtering of signals defined on the unit sphere, as an analogy to joint time-frequency filtering. For this purpose, we first map spherical signals from spatial domain into joint spatio-spectral domain, where a spatio-spectral signal transformation or modification is introduced. For mapping spatial signals into joint spatio-spectral domain, we use the spatially localized spherical harmonic transform (SLSHT) from the literature. We then propose a suitable scheme to transform the modified signal from the spatio-spectral domain back to an admissible signal in the spatial domain using the least squares approach. We also show that the overall action of the SLSHT and spatio-spectral signal modification can be described through a single transformation matrix, which is useful in practice. Finally, we discuss two specific and useful instances of spatially-varying spectral filtering, defined through multiplicative and convolutive modification of the SLSHT distribution, and show through numerical examples their effectiveness in selective spectral filtering of different spatial regions of the signal.**

***Index Terms*—Convolution, filtering, spherical harmonics, 2-sphere (unit sphere).**

I. Introduction

In various fields of physical sciences and engineering the domain of signals under consideration is non-Euclidean. An important class of such signals is those whose domain is spherical and the signal processing applications appear in geodesy [1], cosmology [2], spherical harmonic computerized lighting [3], electromagnetic inverse problems [4], medical image analysis [5], 3D beamforming [6] and wireless channel modeling [7], to name a few. To process such signals, a sensible approach is to devise methods that are similar in spirit to well-known techniques for Euclidean signals, while taking into account the non-trivial differences that exist between the two domains.

Many signal processing techniques have already been extended from Euclidean to spherical domain. Examples include convolution [8]–[10], filtering [5], [11], [12], feature extraction [13], [14] and spectrum estimation [15], [16] for signals defined on the unit sphere. At their core, these techniques process the signal directly either in the spatial spherical domain or in the spectral domain, which is enabled through spherical harmonic transform [4], [8], [15], [17], [18] – the well-known counterpart of the Fourier transform.

However, there are situations where analysis and modification of spherical signals jointly or simultaneously in spatial and spectral domains is required. This is particularly important when we wish to reveal and modify *spatially-varying* spectral contents of signals. For this purpose, spherical harmonic transform is simply not adequate because it cannot reveal "localized" spatial contributions of a signal in the spectral domain. For example, consider the convolutive smoothing in the spatial domain [8], [19], which is equivalent to the multiplication of the signal and filter spherical harmonics in spectral domain. Therefore, the same filter is used for smoothing the signal at all spatial positions and it is not possible to apply a spatially-varying operation in the spectral domain and vice versa. This has motivated us to look for suitable joint *spatio-spectral* signal transformations on the unit sphere.

The closest class of related work is the extension of Euclidean wavelets to spherical wavelets, which enables filtering at different scales [13], [14], [20]–[24]. The theoretical conditions on the invertibility of spherical wavelet transform are presented in [5] and the proposed framework is illustrated using wavelets that provide space-scale decomposition. However, to the best of our knowledge, there exists no framework that directly deals with signal transformations and modifications in joint spatial and spherical harmonic domains (spatio-spectral domain for short) rather than in joint spatial and scale (wavelet) domains.

Interestingly the Euclidean counterpart, namely joint time-frequency signal analysis and filtering, is well established for several decades [25]–[29]. In particular, short-time Fourier transform (STFT) and its variations [26]–[32] have triggered research to generalize the concepts of filtering theory to joint time-frequency domain. Saleh and Subotic presented an interesting and novel approach of time-frequency filtering in [26], where they devised the modification of the STFT representation of signal as masking with the filter function in the time-frequency domain. A similar concept is also adopted in [33] for discrete-time signals and is generalized in [27] for different operations in time-frequency domain.

In this paper, we are interested in extending signal filtering based on the concept of STFT in the time-frequency domain

Manuscript received May 06, 2012; revised July 20, 2012 and September 13, 2012; accepted October 08, 2012. Date of publication October 16, 2012; date of current version January 04, 2013. The associate editor coordinating the review of this manuscript and approving it for publication was Dr. Andrzej Cichocki. This work was supported under the Australian Research Council's Discovery Projects funding scheme (Project DP1094350). The associate editor coordinating the review of this manuscript and approving it for publication was Dr. Andrzej Cichocki.

The authors are with the Research School of Engineering, College of Engineering and Computer Science, The Australian National University, Canberra, Australia (e-mail: zubair.khalid@anu.edu.au; parastoo.sadeghi@anu.edu.au; rodney.kennedy@anu.edu.au; salman.durrani@anu.edu.au).

Color versions of one or more of the figures in this paper are available online at http://ieeexplore.ieee.org.

Digital Object Identifier 10.1109/TSP.2012.2225058

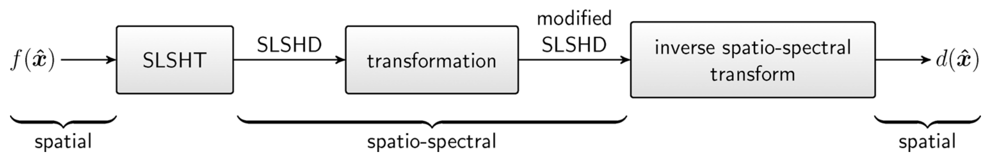

Fig. 1. General schematic for signal transformation via the spatio-spectral domain. The spatial signal, $f(\hat{\boldsymbol{x}})$, on the unit sphere, is first mapped to the spatio-spectral domain using the spatially localized spherical harmonic transform (SLSHT), then its SLSHT distribution (denoted by SLSHD in the figure) is transformed in spatio-spectral domain, and the result is mapped back to the spatial domain using an inverse spatio-spectral transform.

to the joint spatio-spectral domain on the sphere. Fortunately, the basic building block for such signal processing has been developed in the literature. The idea is to apply a set of "windowed" or localized spherical harmonic transforms [34] to the signal of interest. This has been recently coined as spatially localized spherical harmonic transform (SLSHT) and SLSHT distribution in [35], where the effect of different windows on the transformation is studied. In short, SLSHT can be thought of as the spherical counterpart of STFT. The concept of SLSHT has been used for localized spectral analysis [15] and spectral estimation [16] on the sphere. However, the application of SLSHT for signal filtering has not been considered before. In this context, we identify the following open questions:

- Given the SLSHT distribution as a spatio-spectral representation of a signal on the sphere, how can we perform filtering operations on the signal in spatio-spectral domain?
- Once the SLSHT distribution of a signal is modified as a result of processing or filtering in the spatio-spectral domain, how can we obtain a physically valid signal on the sphere that "best" corresponds to the modified spatio-spectral distribution?
- What are the potential candidates for spatio-spectral filtering operations and how can these joint-domain operations be formulated as linear transformations of the signal in spatial or spectral domain?

To address these questions, we consider filtering and modification of signals in the joint spatio-spectral domain. As illustrated in Fig. 1, the SLSHT distribution of the input signal is first obtained, then the SLSHT distribution is processed in the joint spatio-spectral domain to yield the modified distribution and transformed back to the spatial domain using a suitably devised inverse operation. Due to the modification of the SLSHT distribution, there is a possibility that there exists no physical signal which corresponds to the modified distribution—an analogous problem is well known in time-frequency analysis [25]–[29]. Therefore, there is a need to find the signal that best approximates the modified distribution. To summarize, our main contributions in this work are:

1) In Section III, we present a general integral operator that transforms the SLSHT distribution of a signal to a modified spatio-spectral distribution. We also formulate this spatio-spectral modification as a linear transformation of the signal in the spectral domain.
2) For the case when the modified spatio-spectral distribution is not a valid SLSHT distribution, we devise a suitable inverse spatio-spectral transform in Section III-C, which finds a signal whose distribution best approximates the modified distribution in the least squares sense.
3) Using the proposed paradigm of signal transformation, we investigate two types of filtering operations in spatio-spectral domain. First in Section IV-B, we consider filtering as multiplication of the filter function defined in spatio-spectral domain and the given SLSHT distribution. Later in Section IV-C, we perform filtering as convolution of the filter function and the SLSHT distribution of a signal. In contrast to the conventional *spatially-invariant spectral filtering*, these types of filtering operations can be thought as *spatially-varying spectral filtering* of signals in the spatio-spectral domain. Finally, some specific numerical examples are given in Section V.

II. Mathematical Background

In this section, we briefly review some mathematical background for signals defined on the unit sphere and present the basics of SLSHT, which will be extensively used in the rest of the paper.

A. Signals on the 2-Sphere

Let $\mathbb{S}^2$ denote the 2-sphere or unit sphere, which is defined as $\mathbb{S}^2 \triangleq \{\boldsymbol{x} \in \mathbb{R}^3 \colon \|\boldsymbol{x}\| = 1\}$. Two unit-norm vectors on the 2-sphere, such as $\hat{\boldsymbol{x}}$ and $\hat{\boldsymbol{y}}$, can be represented in the spherical coordinates as $\hat{\boldsymbol{x}} \equiv \hat{\boldsymbol{x}}(\theta,\phi) \triangleq (\sin\theta\cos\phi,\, \sin\theta\sin\phi,\, \cos\theta)' \in \mathbb{S}^2$ and $\hat{\boldsymbol{y}} \equiv \hat{\boldsymbol{y}}(\vartheta,\varphi) \triangleq (\sin\vartheta\cos\varphi,\, \sin\vartheta\sin\varphi,\, \cos\vartheta)' \in \mathbb{S}^2$, respectively, where $(\cdot)'$ denotes matrix or vector transpose. $\theta, \vartheta \in [0,\pi]$ represent the co-latitude or elevation measured with respect to the positive z–axis and $\phi, \varphi \in [0, 2\pi)$ represent the longitude or azimuth and are measured with respect to the positive x–axis in the $x-y$ plane.

We consider complex-valued functions, such as $f(\hat{\boldsymbol{x}})$ and $h(\hat{\boldsymbol{x}})$, defined on the unit sphere. The space of square integrable complex functions forms a Hilbert space, denoted by $L^2(\mathbb{S}^2)$, with the inner product defined as

$$\langle f, h\rangle \triangleq \int_{\mathbb{S}^2} f(\hat{\boldsymbol{x}})\,\overline{h(\hat{\boldsymbol{x}})}\,ds(\hat{\boldsymbol{x}}), \tag{1}$$

where $ds(\hat{\boldsymbol{x}}) = \sin\theta\, d\theta\, d\phi$ is the area element, $\overline{(\cdot)}$ denotes complex conjugate and the integration is carried out over the whole unit sphere. The inner product in (1) induces a norm $\|f\| \triangleq \langle f, f\rangle^{\frac{1}{2}}$. Throughout this paper, functions with finite induced norm belonging to $L^2(\mathbb{S}^2)$ are referred as signals on the sphere or signals for short.

The Hilbert space $L^2(\mathbb{S}^2)$ is separable and spherical harmonic functions (or spherical harmonics for short) $Y_\ell^m(\hat{\boldsymbol{x}}) = Y_\ell^m(\theta,\phi)$ [4], [17] of all degrees $\ell \geq 0$ and orders $-\ell \leq m \leq \ell$ form the archetype complete orthonormal set of basis functions. By completeness, any signal $f \in L^2(\mathbb{S}^2)$ can be expanded as

$$f(\hat{\boldsymbol{x}}) = \sum_{\ell=0}^{\infty} \sum_{m=-\ell}^{\ell} (f)_\ell^m Y_\ell^m(\hat{\boldsymbol{x}}), \tag{2}$$

where

$$(f)_\ell^m \triangleq \langle f, Y_\ell^m \rangle = \int_{\mathbb{S}^2} f(\hat{\boldsymbol{x}}) \overline{Y_\ell^m(\hat{\boldsymbol{x}})}\, ds(\hat{\boldsymbol{x}}) \tag{3}$$

is the spherical harmonic Fourier coefficient (or spherical harmonic coefficient for short) of degree ℓ and order m. Some background properties of spherical harmonics used in this work are given in Appendix A. For notational simplifications, we may express the spherical harmonic Y_ℓ^m as Y_n and spherical harmonic coefficient $(f)_\ell^m$ as $(f)_n$. That is, as a function of a single integer index n instead of two integer indices ℓ and m, using the *one-to-one* mapping

$$\begin{aligned} &(\ell, m) \leftrightarrow n, \quad n = \ell^2 + \ell + m, \\ &\ell = \lfloor \sqrt{n} \rfloor, \quad m = n - \lfloor \sqrt{n} \rfloor (\lfloor \sqrt{n} \rfloor - 1), \end{aligned} \tag{4}$$

where $\lfloor \cdot \rfloor$ denotes the integer floor function.

B. Important Subspaces of $L^2(\mathbb{S}^2)$

The set of *bandlimited* signals, such as $f(\hat{\boldsymbol{x}}) \in L^2(\mathbb{S}^2)$, with the maximum spectral degree L_f such that $(f)_\ell^m = 0$ for $\ell > L_f$ forms a subspace of $L^2(\mathbb{S}^2)$ and is denoted by $\mathcal{H}_{L_f}$.

The set of azimuthally symmetric functions which are independent of the azimuth angle (such that $f(\hat{\boldsymbol{x}}) = f(\theta, \phi) = f(\theta)$) forms a subspace of $L^2(\mathbb{S}^2)$ and is denoted by $\mathcal{H}^0$. In this case, only zero-order spherical harmonic coefficients of f are non-zero. That is $(f)_\ell^m = 0$ for all $m \neq 0$.

C. Important Operators on $L^2(\mathbb{S}^2)$

1) Spherical Harmonic (Fourier) Transform: Define the operator $\mathcal{F}$, which transforms the signal $f(\hat{\boldsymbol{x}})$ in the spatial domain to the signal in spectral domain, where the *spectral response* is denoted by $\boldsymbol{f} = \big((f)_0, (f)_1, (f)_2, \ldots\big)'$ and the operation is represented by

$$\boldsymbol{f} = \big(\mathcal{F} f\big)(\hat{\boldsymbol{x}}).$$

Also the inverse spherical harmonic transform $\mathcal{F}^{-1}$ is well-defined such that $\mathcal{F}^{-1}\boldsymbol{f} = f(\hat{\boldsymbol{x}})$. If $f(\hat{\boldsymbol{x}})$ is bandlimited belonging to $\mathcal{H}_{L_f}$, then $\boldsymbol{f} = \big((f)_0, (f)_1, (f)_2, \ldots, (f)_{N_f}\big)'$, where $N_f = L_f^2 + 2L_f$.

2) Rotation: Define the rotation operator $\mathcal{D}(\varphi, \vartheta, \omega)$, which rotates the function on the sphere in a sequence of $\omega \in [0, 2\pi)$ rotation around z–axis, then $\vartheta \in [0, \pi]$ rotation about y–axis followed by a $\varphi \in [0, 2\pi)$ rotation around z–axis. The rotation angles are referred to as the Euler angles. Under the rotation operation $\mathcal{D}(\varphi, \vartheta, \omega)$, the spherical harmonic coefficients of the rotated signal are related to those of the original signal through [17]

$$\begin{aligned} \big(\mathcal{D}(\varphi, \vartheta, \omega) f\big)_\ell^m &\triangleq \big\langle \mathcal{D}(\varphi, \vartheta, \omega) f, Y_\ell^m \big\rangle \\ &= \sum_{m'=-\ell}^{\ell} D_\ell^{m,m'}(\varphi, \vartheta, \omega) (f)_\ell^{m'}, \end{aligned} \tag{5}$$

where $D_\ell^{m,m'}(\varphi, \vartheta, \omega)$ is Wigner-D function [17] and is given by

$$D_\ell^{m,m'}(\varphi, \vartheta, \omega) = e^{-im\varphi} d_\ell^{m,m'}(\vartheta)\, e^{-im'\omega}, \tag{6}$$

and $d_\ell^{m,m'}(\vartheta)$ denotes the Wigner-d function [17] and its explicit expression is provided in Appendix A. We note that by factoring of a single rotation into two rotations, as proposed in [36] and applied in [13], [18], [37], [38], the Wigner-D function can be computed efficiently by using FFTs over all three Euler angles.

For the azimuthally symmetric functions $h(\hat{\boldsymbol{x}}) \in \mathcal{H}^0$, the ω rotation around z–axis becomes ineffective and can be set to $\omega = 0$. Hence, the expression in (5) simplifies to

$$\begin{aligned} \big(\mathcal{D}(\varphi, \vartheta, 0) h\big)_\ell^m &= D_\ell^{m,0}(\varphi, \vartheta, 0)(h)_\ell^0 \\ &= \sqrt{\frac{4\pi}{2\ell+1}}\, \overline{Y_\ell^m(\vartheta, \varphi)} (h)_\ell^0, \end{aligned} \tag{7}$$

where the second equality follows from the following relation

$$D_\ell^{m,0}(\varphi, \vartheta, 0) = \sqrt{\frac{4\pi}{2\ell+1}}\, \overline{Y_\ell^m(\vartheta, \varphi)}. \tag{8}$$

3) Convolution: There are different definitions of spherical convolution available in the literature [5], [9], [10]. For the purpose of this paper, it suffices to consider the following definition of convolution

$$\big(h \circledast f\big)(\hat{\boldsymbol{y}}) = \int_{\mathbb{S}^2} \big(\mathcal{D}(\varphi, \vartheta, 0) h\big)(\hat{\boldsymbol{x}})\, f(\hat{\boldsymbol{x}})\, ds(\hat{\boldsymbol{x}}), \tag{9}$$

where the two rotation angles (ϑ, φ) parameterize the point $\hat{\boldsymbol{y}} = \hat{\boldsymbol{y}}(\vartheta, \varphi)$ on the 2-sphere. This definition is adapted from the definition of convolution in [5], but unlike the general case in [5], the output domain of the convolution remains in $L^2(\mathbb{S}^2)$. If the kernel $h(\hat{\boldsymbol{x}}) \in \mathcal{H}^0$ is azimuthally symmetric, then (9) becomes an isotropic convolution which is predominantly used in this paper. In this case, the spherical harmonic of the output $\big(h \circledast f\big)_\ell^m$ is given by [8]–[10]

$$(h \circledast f)_\ell^m = \sqrt{\frac{4\pi}{2\ell+1}} (h)_\ell^0 (f)_\ell^m. \tag{10}$$

D. Spatially Localized Spherical Harmonics Transform (SLSHT)

Analogous to short-time Fourier transform (STFT), SLSHT has been defined as a set of *windowed spherical harmonic transforms* in [34], [35] to represent the signal jointly in the spatio-spectral domain. The core idea is simple. An azimuthally symmetric window function $h(\hat{\boldsymbol{x}}) \in \mathcal{H}^0$ (nominally concentrated around the north pole) is first rotated by $(\varphi, \vartheta, 0)$, where (ϑ, φ) parametrize the point $\hat{\boldsymbol{y}} = \hat{\boldsymbol{y}}(\vartheta, \varphi)$ on the 2-sphere. Then the rotated kernel $\big(\mathcal{D}(\varphi, \vartheta, 0) h\big)(\hat{\boldsymbol{x}})$ *multiplies* the desired signal $f(\hat{\boldsymbol{x}})$ and finally, the spherical harmonic Fourier transform is applied to the multiplied signal $\big(\mathcal{D}(\varphi, \vartheta, 0) h\big)(\hat{\boldsymbol{x}}) f(\hat{\boldsymbol{x}})$. That is, the SLSHT attempts to reveal the contribution of spherical harmonics localized around $\hat{\boldsymbol{y}}$. Mathematically, the SLSHT evaluated at point $\hat{\boldsymbol{y}} = \hat{\boldsymbol{y}}(\vartheta, \varphi)$, degree ℓ and order m is defined as

$$\begin{aligned} g(\hat{\boldsymbol{y}}; \ell, m) &= g(\hat{\boldsymbol{y}}; n) \\ &\triangleq \int_{\mathbb{S}^2} \big(\mathcal{D}(\varphi, \vartheta, 0) h\big)(\hat{\boldsymbol{x}}) f(\hat{\boldsymbol{x}}) \overline{Y_\ell^m(\hat{\boldsymbol{x}})}\, ds(\hat{\boldsymbol{x}}), \\ \hat{\boldsymbol{y}} &= \hat{\boldsymbol{y}}(\vartheta, \varphi),\ (\ell, m) \leftrightarrow n. \end{aligned} \tag{11}$$

The SLSHT is dependent on the chosen window h, but for brevity, this dependence is not explicit in the notation. We emphasize that unlike spherical harmonic coefficient of the signal $f(\hat{\boldsymbol{x}})$, $(f)_\ell^m$, which is only a function of degree ℓ and order m, the SLSHT provides a spatially-varying spherical harmonic representation of the signal (i.e., $g(\hat{\boldsymbol{y}}; \ell, m)$ is a function of the spatial localization $\hat{\boldsymbol{y}}$ and degree and order).

In this paper, we are interested in the case where both signal $f(\hat{\boldsymbol{x}})$ and SLSHT window kernel $h(\hat{\boldsymbol{x}})$ are bandlimited. Let us assume that $f(\hat{\boldsymbol{x}}) \in \mathcal{H}_{L_f}$ and $h(\hat{\boldsymbol{x}}) \in \mathcal{H}_{L_h}$ (since the kernel is assumed to be azimuthally symmetric, $h(\hat{\boldsymbol{x}}) \in \mathcal{H}_{L_h}^0 \subset \mathcal{H}^0$ would be a more precise notation). In this case, the SLSHT *distribution* $\boldsymbol{g}(\hat{\boldsymbol{y}})$, which represents the signal f in joint spatio-spectral domain using SLSHT is given by

$$\boldsymbol{g}(\hat{\boldsymbol{y}}) \triangleq \big(g(\hat{\boldsymbol{y}}; 0),\, g(\hat{\boldsymbol{y}}; 1),\, g(\hat{\boldsymbol{y}}; 2),\, \ldots,\, g(\hat{\boldsymbol{y}}; N_g)\big)', \tag{12}$$

where $N_g = L_g^2 + 2L_g$ and $L_g = L_f + L_h$. Specializing (7) for the SLSHT window kernel h at point $\hat{\boldsymbol{y}} = \hat{\boldsymbol{y}}(\vartheta, \varphi)$, we define

$$\begin{aligned} (h)_r(\hat{\boldsymbol{y}}) &\triangleq \langle \mathcal{D}(\varphi, \vartheta, 0) h, Y_r \rangle = \sqrt{\frac{4\pi}{2p+1}}\, \overline{Y_p^q(\hat{\boldsymbol{y}})} (h)_p^0, \\ \hat{\boldsymbol{y}} &= \hat{\boldsymbol{y}}(\vartheta, \varphi), \quad (p, q) \leftrightarrow r. \end{aligned} \tag{13}$$

Using (13), (2), (3) and the mapping $(s, t) \leftrightarrow u$, we can alternatively write $g(\hat{\boldsymbol{x}}; n)$ in (11) as

$$g(\hat{\boldsymbol{y}}; n) = \sum_{u=0}^{N_f} (f)_u \sum_{r=0}^{N_h} (h)_r(\hat{\boldsymbol{y}})\, T(u; r; n), \tag{14}$$

where $N_h = L_h^2 + 2L_h$ and

$$T(u; r; n) = T(r; u; n) \triangleq \int_{\mathbb{S}^2} Y_r(\hat{\boldsymbol{x}}) Y_u(\hat{\boldsymbol{x}}) \overline{Y_n(\hat{\boldsymbol{x}})}\, ds(\hat{\boldsymbol{x}}) \tag{15}$$

denotes the spherical harmonic triple product and its explicit expression is provided in Appendix A. Using the preceding formulation, the SLSHT distribution $\boldsymbol{g}(\hat{\boldsymbol{y}})$ in (12) can be written in matrix form as

$$\boldsymbol{g}(\hat{\boldsymbol{y}}) = \boldsymbol{\Psi}(\hat{\boldsymbol{y}}) \boldsymbol{f}, \tag{16}$$

where $\boldsymbol{f} = \big(\mathcal{F} f\big)(\hat{\boldsymbol{x}})$ and $\boldsymbol{\Psi}$ is the transformation operator matrix of size $(N_g + 1) \times (N_f + 1)$, which projects the given signal in spectral domain to the spatio-spectral domain and its entries are given by

$$\psi_{n,u}(\hat{\boldsymbol{y}}) = \sum_{r=0}^{N_h} (h)_r(\hat{\boldsymbol{y}})\, T(u; r; n). \tag{17}$$

The n-th spherical harmonic coefficient of the signal $f(\hat{\boldsymbol{x}})$ can be obtained as the spherical harmonic marginal of $g(\hat{\boldsymbol{x}}; n)$. That is, by integrating $g(\hat{\boldsymbol{x}}; n)$ over the spatial domain [34], [35]

$$(f)_n = \frac{1}{K} \int_{\mathbb{S}^2} g(\hat{\boldsymbol{y}}; n)\, ds(\hat{\boldsymbol{y}}), \tag{18}$$

where $K = \sqrt{4\pi}\,(h)_0^0$ is a factor that depends on the SLSHT window kernel h. More concisely, we can write

$$\boldsymbol{f} = \frac{1}{K} \int_{\mathbb{S}^2} \boldsymbol{g}(\hat{\boldsymbol{y}})\, ds(\hat{\boldsymbol{y}}). \tag{19}$$

Remark 1: We are using a bandlimited window function to capture the localized contribution of spherical harmonics. Therefore, from the uncertainty principle, the window function cannot be spatially limited. However it must be concentrated in the desired localization region in order to minimize the contribution of signal outside the localized spatial region [35]. The bandlimited spatially concentrated eigenfunction obtained from Slepian concentration problem on the sphere [1], [15], [39] is proposed as suitable window functions for the SLSHT in [35], since they attain the lower bound imposed by the uncertainty principle [20], [40].

III. Signal Transformation in Spatio-Spectral Domain

In the previous section, we saw that the SLSHT distribution represents the spatially-varying spectral representation of a signal as a function of both spatial location $\hat{\boldsymbol{y}}$ and degree and order ℓ, m. As a result, it offers the opportunity to transform, modify and filter the signal in the joint spatio-spectral domain, which can be very useful for the processing of signals that contain spatially-varying spectral contents. In this section, we use the SLSHT distribution to address questions 1 and 2 posed in the introduction. Here, we use a general integral operator approach to transform the SLSHT distribution. Later in Sections IV and V, we specify two types of transformations and analyze their properties and usefulness.

For this purpose, we use a set of $N_g + 1$ kernels defined on domain $\mathbb{S}^2 \times \mathbb{S}^2$ and denoted by $\boldsymbol{\zeta}(\hat{\boldsymbol{x}}, \hat{\boldsymbol{y}}; n)$. Each kernel is used to operate on its corresponding SLSHT component $g(\hat{\boldsymbol{y}}; n)$ as follows

$$v(\hat{\boldsymbol{x}}; n) = \int_{\mathbb{S}^2} \zeta(\hat{\boldsymbol{x}}, \hat{\boldsymbol{y}}; n)\, g(\hat{\boldsymbol{y}}; n)\, ds(\hat{\boldsymbol{y}}), \quad 0 \le n \le N_g \tag{20}$$

to generate a modified component $v(\hat{\boldsymbol{x}}; n)$ in the spatio-spectral domain. For a given $\hat{\boldsymbol{x}}$ and $\hat{\boldsymbol{y}}$ and by arranging all the kernels in vector form as

$$\boldsymbol{\zeta}(\hat{\boldsymbol{x}}, \hat{\boldsymbol{y}}) \triangleq \big(\zeta(\hat{\boldsymbol{x}}, \hat{\boldsymbol{y}}; 0),\, \zeta(\hat{\boldsymbol{x}}, \hat{\boldsymbol{y}}; 1),\, \ldots,\, \zeta(\hat{\boldsymbol{x}}, \hat{\boldsymbol{y}}; N_g)\big)',$$

we can write the overall operation on the SLSHT distribution in a concise form given below

$$\boldsymbol{v}(\hat{\boldsymbol{x}}) = \big(\mathcal{K}\boldsymbol{g}\big)(\hat{\boldsymbol{x}}) \triangleq \int_{\mathbb{S}^2} \boldsymbol{\zeta}(\hat{\boldsymbol{x}}, \hat{\boldsymbol{y}}) \odot \boldsymbol{g}(\hat{\boldsymbol{y}})\, ds(\hat{\boldsymbol{y}}), \tag{21}$$

where $\odot$ denotes component-wise operation of the kernel elements in $\boldsymbol{\zeta}(\hat{\boldsymbol{x}}, \hat{\boldsymbol{y}})$ on corresponding SLSHT components in $\boldsymbol{g}(\hat{\boldsymbol{y}})$. Note that the kernels $\zeta(\hat{\boldsymbol{x}}, \hat{\boldsymbol{y}}; n)$ for $N_v < n \le N_g$ can be zero and hence, in general the "effective" length of the modified distribution $\boldsymbol{v}(\hat{\boldsymbol{x}})$ satisfies $N_v+1 \leq N_g+1$. Nevertheless for consistency with the transformation operator matrix $\boldsymbol{\Psi}$, we will deal with a full-length modified distribution $\boldsymbol{v}(\hat{\boldsymbol{x}})$ of length N_g+1, even though some of its last components may be zero. We also note that while $\boldsymbol{v}(\hat{\boldsymbol{x}})$ is a form of modified spatio-spectral distribution, it is not necessarily a valid SLSHT distribution. This will be further elaborated shortly.

Using the formulation of SLSHT distribution in (16), we can relate the modified distribution (21) to the vector spectral representation of the signal, $\boldsymbol{f}$, and the SLSHT distribution transformation operator matrix $\boldsymbol{\Psi}(\hat{\boldsymbol{y}})$ as

$$\boldsymbol{v}(\hat{\boldsymbol{x}}) = \big(\mathcal{K}\boldsymbol{\Psi}\big)(\hat{\boldsymbol{x}})\boldsymbol{f} = \left(\int_{\mathbb{S}^2} \mathrm{diag}\big(\boldsymbol{\zeta}(\hat{\boldsymbol{x}},\hat{\boldsymbol{y}})\big)\boldsymbol{\Psi}(\hat{\boldsymbol{y}})\,ds(\hat{\boldsymbol{y}})\right)\boldsymbol{f}, \tag{22}$$

where $\mathrm{diag}\big(\boldsymbol{\zeta}(\hat{\boldsymbol{x}},\hat{\boldsymbol{y}})\big)$ returns the diagonal matrix with diagonal entries specified by the vector $\boldsymbol{\zeta}(\hat{\boldsymbol{x}},\hat{\boldsymbol{y}})$.

Remark 2: In the formulation of spatio-spectral transformation of signal in (21), we note that $\boldsymbol{g}(\hat{\boldsymbol{y}})$ can be any representation of signals in spatio-spectral domain. However, here, we are specifically considering SLSHT distribution as the signal representation in spatio-spectral domain.

A. Exact Inverse Spatio-Spectral Transform

We note that not every spatio-spectral distribution, $\boldsymbol{v}(\hat{\boldsymbol{x}})$, is a valid SLSHT distribution. In other words, it is possible that there exists no signal belonging to $L^2(\mathbb{S}^2)$ for which $\boldsymbol{v}(\hat{\boldsymbol{x}})$ is its corresponding SLSHT distribution. An obvious example would be a spatio-spectral distribution truncated both in spatial and spectral domains. From the uncertainty principle, one can expect that there exists no signal which corresponds to this type of modified distribution.

But first, let us assume that the modified distribution vector $\boldsymbol{v}(\hat{\boldsymbol{x}})$ is indeed a valid SLSHT distribution. Then there exists a signal $d(\hat{\boldsymbol{x}}) \in L^2(\mathbb{S}^2)$ with spectral response $\boldsymbol{d}$ corresponding to $\boldsymbol{v}(\hat{\boldsymbol{x}})$, which can be recovered through the "inversion formula" (18) as

$$(d)_u = \frac{1}{K}\int_{\mathbb{S}^2} v(\hat{\boldsymbol{y}};u)\,ds(\hat{\boldsymbol{y}}). \tag{23}$$

Applying this back into (14) results in the following admissibility condition

$$\begin{aligned} v(\hat{\boldsymbol{x}};n) &= \frac{1}{K}\sum_{u=0}^{N_f}(d)_u\sum_{r=0}^{N_h}(h)_r(\hat{\boldsymbol{x}})\,T(u;r;n) \\ &= \frac{1}{K}\sum_{u=0}^{N_f}\sum_{r=0}^{N_h}(h)_r(\hat{\boldsymbol{x}})\,T(u;r;n)\int_{\mathbb{S}^2} v(\hat{\boldsymbol{y}};u)\,ds(\hat{\boldsymbol{y}}). \end{aligned} \tag{24}$$

The admissibility condition in (24) is expressed on the modified distribution $v(\hat{\boldsymbol{x}};n)$. By using the definition of SLSHT distribution in (16), the formulation of modified distribution $\boldsymbol{v}(\hat{\boldsymbol{x}})$ in (22) and the inversion relation in (19), we can also express the admissibility condition on the set of kernels $\boldsymbol{\zeta}(\hat{\boldsymbol{x}},\hat{\boldsymbol{y}})$ as

$$\begin{aligned} &K\int_{\mathbb{S}^2}\mathrm{diag}\big(\boldsymbol{\zeta}(\hat{\boldsymbol{x}},\hat{\boldsymbol{y}})\big)\boldsymbol{\Psi}(\hat{\boldsymbol{y}})\,ds(\hat{\boldsymbol{y}}) \\ &\quad = \boldsymbol{\Psi}(\hat{\boldsymbol{x}})\left(\int_{\mathbb{S}^2}\int_{\mathbb{S}^2}\mathrm{diag}\big(\boldsymbol{\zeta}(\hat{\boldsymbol{x}},\hat{\boldsymbol{y}})\big)\boldsymbol{\Psi}(\hat{\boldsymbol{y}})\,ds(\hat{\boldsymbol{x}})ds(\hat{\boldsymbol{y}})\right). \end{aligned} \tag{25}$$

If the modified distribution satisfies the condition in (24) or the set of kernels $\boldsymbol{\zeta}(\hat{\boldsymbol{x}},\hat{\boldsymbol{y}})$ are chosen to satisfy the condition in (25), we can find a signal $d(\hat{\boldsymbol{x}}) = \mathcal{F}^{-1}\boldsymbol{d}$, such that $\boldsymbol{v}(\hat{\boldsymbol{x}}) = \boldsymbol{\Psi}(\hat{\boldsymbol{x}})\boldsymbol{d}$. We remind ourselves that according to the discussion following (21), the effective length of $\boldsymbol{d}$, N_d+1, can be smaller than N_f+1. For example, if we choose each kernel $\zeta(\hat{\boldsymbol{x}},\hat{\boldsymbol{y}};n)$ as bandlimited Dirac-delta function given by

$$\zeta(\hat{\boldsymbol{x}},\hat{\boldsymbol{y}};n) = K_n\sum_{u=0}^{N_{\zeta_n}} Y_u(\hat{\boldsymbol{x}})\overline{Y_u(\hat{\boldsymbol{y}})}, \tag{26}$$

where $N_h \leq N_{\zeta_n} < \infty$ and K_n denotes any complex number, the set of kernels $\boldsymbol{\zeta}(\hat{\boldsymbol{x}},\hat{\boldsymbol{y}})$ satisfies the condition in (25) and the modified distribution distribution $\boldsymbol{v}(\hat{\boldsymbol{x}})$ is a valid SLSHT distribution of the signal d such that $(d)_u = K_u(f)_u$. The choice of kernel in (26) is the simplest case and we note that any set of kernels which satisfies the admissibility condition results in a valid SLSHT distribution $\boldsymbol{v}(\hat{\boldsymbol{x}})$.

B. Least Squares Solution

For the case that the modified distribution $\boldsymbol{v}(\hat{\boldsymbol{x}})$ is not a valid SLSHT distribution, we seek to solve an optimization problem to find a signal $d(\hat{\boldsymbol{x}}) \in L^2(\mathbb{S}^2)$ having the spectral response $\boldsymbol{d} = \big(\mathcal{F}\,d\big)(\hat{\boldsymbol{x}})$ and the SLSHT distribution $\boldsymbol{\Psi}(\hat{\boldsymbol{x}})\boldsymbol{d}$, which approximates $\boldsymbol{v}(\hat{\boldsymbol{x}})$ in least squares sense. For this purpose, we define the error term

$$e(\hat{\boldsymbol{x}};n) \triangleq v(\hat{\boldsymbol{x}};n) - \Psi_{n,:}(\hat{\boldsymbol{x}})\boldsymbol{d},$$

where $\Psi_{n,:}(\hat{\boldsymbol{x}})$ is the n-th row of $\boldsymbol{\Psi}(\hat{\boldsymbol{x}})$. The total error is then

$$E = \big\|\boldsymbol{v}-\boldsymbol{\Psi}\boldsymbol{d}\big\|^2 \triangleq \int_{\mathbb{S}^2}\sum_{n=0}^{N_g}\big|e(\hat{\boldsymbol{x}};n)\big|^2\,ds(\hat{\boldsymbol{x}}), \tag{27}$$

where the norm is, in fact, the norm of vectors in the spatio-spectral domain. Setting the gradient of E with respect to $\boldsymbol{d}$ to zero will result in the least squares approximate solution and we summarize this in the following theorem, which is also shown in Fig. 2.

Theorem 1 (Least Squares Solution): Let the SLSHT distribution $\boldsymbol{g}(\hat{\boldsymbol{y}}) = \boldsymbol{\Psi}(\hat{\boldsymbol{y}})\,\boldsymbol{f}$, as defined in (12)–(17), be modified into $\boldsymbol{v}(\hat{\boldsymbol{x}})$ according to (20)–(21). The signal $\boldsymbol{d}(\hat{\boldsymbol{x}}) \in L^2(\mathbb{S}^2)$ that best describes $\boldsymbol{v}(\hat{\boldsymbol{x}})$ in the least squares sense has its spectral response defined through

$$\boldsymbol{d} \triangleq \arg\min_{\widetilde{\boldsymbol{d}}}\big\|\boldsymbol{v}-\boldsymbol{\Psi}\widetilde{\boldsymbol{d}}\big\|^2, \tag{28}$$

and is found to be

$$\boldsymbol{d} = \frac{1}{\mathcal{E}}\int_{\mathbb{S}^2}\boldsymbol{\Psi}^H(\hat{\boldsymbol{x}})\,\boldsymbol{v}(\hat{\boldsymbol{x}})\,ds(\hat{\boldsymbol{x}}), \tag{29}$$

where $(\cdot)^H$ denotes Hermitian transpose and $\mathcal{E}$ is defined as the energy of the window kernel h given by

$$\mathcal{E} \triangleq \langle h,h\rangle = \sum_{p=0}^{L_h}\big|(h)_p^0\big|^2. \tag{30}$$

Proof: See Appendix B. ■

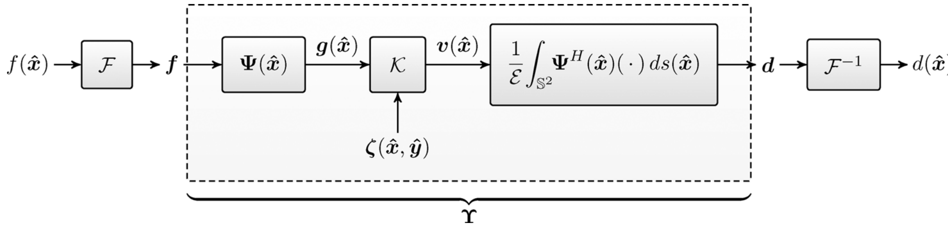

Fig. 2. Spatio-spectral processing: $\boldsymbol{f} = \big(\mathcal{F}f\big)(\hat{\boldsymbol{x}})$ is the spectral response of the signal $f(\hat{\boldsymbol{x}})$ on the unit sphere, $\boldsymbol{g}(\hat{\boldsymbol{x}})$ is corresponding SLSHT distribution in the spatio-spectral domain, $\boldsymbol{v}(\hat{\boldsymbol{x}})$ is the modified SLSHT distribution under operator $\mathcal{K}$ with kernel $\boldsymbol{\zeta}(\hat{\boldsymbol{x}},\hat{\boldsymbol{y}})$ in the spatio-spectral domain, and $\boldsymbol{d}$ is the spectral response of the output signal $d(\hat{\boldsymbol{x}})$ on the unit sphere. The transformation between the spectral responses is linear and given by the spatio-spectral transformation matrix $\boldsymbol{\Upsilon}$.

Corollary 1: If the modified distribution is a valid SLSHT distribution, by plugging $\boldsymbol{v}(\hat{\boldsymbol{x}}) = \boldsymbol{\Psi}(\hat{\boldsymbol{x}})\boldsymbol{d}$ into (29) and following the mathematical details provided Appendix B, it is easy to verify that Theorem 1 becomes the exact solution.

C. Spatio-Spectral Transformation as Linear Transformation

From Fig. 2, it becomes clear that we can express the overall process of transforming the bandlimited signal with spectral response $\boldsymbol{f}$, with the maximum spectral degree L_f, to another bandlimited signal $\boldsymbol{d}$ according to the following linear transformation

$$\boldsymbol{d} = \boldsymbol{\Upsilon}\,\boldsymbol{f} \tag{31}$$

where $\boldsymbol{\Upsilon}$ is a matrix of size $(N_f+1)\times(N_f+1)$ and is referred to as the spatio-spectral transformation matrix as shown in Fig. 2. This transformation matrix is useful, because in a single step it encapsulates 1) projection of $\boldsymbol{f}$ into the spatio-spectral domain to obtain $\boldsymbol{g}(\hat{\boldsymbol{x}})$, 2) processing in the spatio-spectral domain which yields $\boldsymbol{v}(\hat{\boldsymbol{x}})$, and 3) transformation from the spatio-spectral domain back to spectral domain to obtain $\boldsymbol{d}$. Therefore, knowing $\boldsymbol{\Upsilon}$ is enough for spatio-spectral transformation of $\boldsymbol{f}$. Using the result in Theorem 1, the formulation of modified distribution in (22) and the SLSHT distribution expression in (16), we can express $\boldsymbol{\Upsilon}$ as

$$\boldsymbol{\Upsilon} = \frac{1}{\mathcal{E}}\int_{\mathbb{S}^2}\int_{\mathbb{S}^2}\boldsymbol{\Psi}^H(\hat{\boldsymbol{x}})\big(\mathrm{diag}\big(\boldsymbol{\zeta}(\hat{\boldsymbol{x}},\hat{\boldsymbol{y}})\big)\boldsymbol{\Psi}(\hat{\boldsymbol{y}})\big)\,ds(\hat{\boldsymbol{y}})\,ds(\hat{\boldsymbol{x}}), \tag{32}$$

which depends on the kernel vector $\boldsymbol{\zeta}(\hat{\boldsymbol{x}},\hat{\boldsymbol{y}})$ and the SLSHT distribution operator matrix $\boldsymbol{\Psi}(\hat{\boldsymbol{x}})$. Since $\boldsymbol{\Psi}(\hat{\boldsymbol{x}})$ depends on the chosen window function used for spatial localization, the kernel and the window function completely characterize the spatio-spectral transformation and processing of signals in the proposed framework.

IV. Filtering in Spatio-Spectral Domain

In the previous section, we provided a general framework for modification of the SLSHT distribution using integral operators and discussed how the modified distribution can be transformed back to a valid signal on the sphere. In this section, we address the third question posed in the introduction. That is, we aim to study specific, but useful types of signal filtering in joint spatio-spectral domain. The filtering can be either taken as multiplication or convolution of the filter function and the SLSHT distribution in the spatio-spectral domain, which will be discussed in the following two subsections. But first, we define the filter function in spatio-spectral domain that modifies the given SLSHT distribution of a signal.

Definition 1 (Filter Function in Spatio-Spectral Domain): Define $\boldsymbol{z}(\hat{\boldsymbol{x}})$ to be the filter function in spatio-spectral domain as

$$\boldsymbol{z}(\hat{\boldsymbol{x}}) \triangleq \big(z(\hat{\boldsymbol{x}};0), z(\hat{\boldsymbol{x}};1), z(\hat{\boldsymbol{x}};2), \ldots, z(\hat{\boldsymbol{x}};N_g)\big)', \tag{33}$$

where each element $z(\hat{\boldsymbol{x}};n)$ for $0 \le n \le N_g$ can be a finite-norm, square integrable function on the unit sphere with the maximum spectral degree L_{z_n} and spherical harmonic expansion $z(\hat{\boldsymbol{x}};n) = \sum_{c=0}^{N_{z_n}}(z_n)_c Y_c(\hat{\boldsymbol{x}})$, where $N_{z_n} = L_{z_n}^2 + 2L_{z_n}$. The spectral response of each component of the filter function is defined as $\boldsymbol{z}_n \triangleq \big((z_n)_0,\, (z_n)_1,\, \ldots,\, (z_n)_{N_{z_n}}\big) \triangleq \big(\mathcal{F}z\big)(\hat{\boldsymbol{x}};n)$.

We use the definition of signal transformation in the joint spatio-spectral domain using the operator $\mathcal{K}$ as defined in (21) and relate the kernel $\boldsymbol{\zeta}(\hat{\boldsymbol{x}},\hat{\boldsymbol{y}})$ to the filter function $\boldsymbol{z}(\hat{\boldsymbol{x}})$ to define filtering operations in joint spatio-spectral domain. The modified distribution $\boldsymbol{v}(\hat{\boldsymbol{x}})$, which is obtained as either multiplication or convolution of the filter function and the SLSHT distribution of the signal, may not be a valid SLSHT distribution and it may not be possible to find the signal $d(\hat{\boldsymbol{x}})$, which exactly describes the distribution $\boldsymbol{v}(\hat{\boldsymbol{x}})$. Thus, the approximate approach as mentioned in Theorem 1 can be employed to determine the signal $d(\hat{\boldsymbol{x}})$, whose SLSHT distribution is closest to the modified distribution in the least squares sense.

In the following two subsections, we define multiplicative and convolutive filtering operations in spatio-spectral domain, respectively and formulate the expressions to determine the signal $d(\hat{\boldsymbol{x}})$ from the modified distribution $\boldsymbol{v}(\hat{\boldsymbol{x}})$. We also present the proposed filtering operations as linear transformations of the signal as given in (31) and provide specific expressions for the spatio-spectral transformation matrix $\boldsymbol{\Upsilon}$ in (32) for these two types of filtering operations.

A. Multiplicative Modification of SLSHT Distribution

In the time-frequency analysis, a time-domain signal can be filtered in joint time-frequency domain through multiplication of its time-frequency representation and the filter function as described in [26]–[30], [33], [41]. Using SLSHT distribution as spatio-spectral representation of a signal on the sphere, we define an analogous multiplicative filtering in joint spatio-spectral domain.

Definition 2 (Multiplicative SLSHT Modification): Relating the kernel $\boldsymbol{\zeta}(\hat{\boldsymbol{x}},\hat{\boldsymbol{y}})$ in (21) to the filter function $\boldsymbol{z}(\hat{\boldsymbol{x}})$ as

$$\boldsymbol{\zeta}(\hat{\boldsymbol{x}},\hat{\boldsymbol{y}}) \triangleq \boldsymbol{z}(\hat{\boldsymbol{x}})\,\delta(\hat{\boldsymbol{x}},\hat{\boldsymbol{y}}), \tag{34}$$

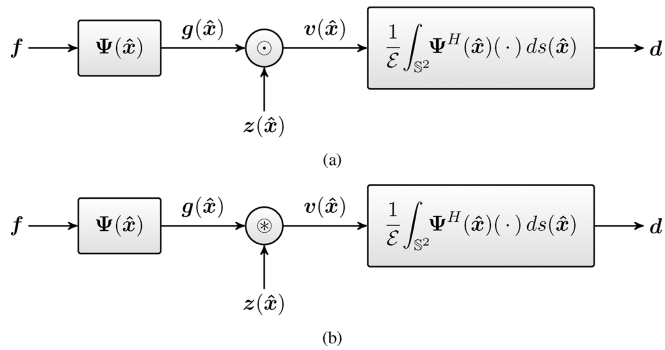

Fig. 3. Block diagram that represents the concept of filtering in spatio-spectral domain as (a) multiplicative modification of the SLSHT distribution and (b) convolutive modification of the SLSHT distribution.

where $\delta(\hat{\boldsymbol{x}}, \hat{\boldsymbol{y}})$ is the Dirac delta function on the sphere (See Appendix A, (62)), we define component-wise multiplication of the SLSHT distribution $\boldsymbol{g}(\hat{\boldsymbol{x}})$ and the filter function $\boldsymbol{z}(\hat{\boldsymbol{x}})$ to obtain the multiplicative modified distribution (MMD), $\boldsymbol{v}(\hat{\boldsymbol{x}})$ through

$$v(\hat{\boldsymbol{x}}; n) \triangleq z(\hat{\boldsymbol{x}}; n)\, g(\hat{\boldsymbol{x}}; n), \tag{35}$$

for $0 \leq n \leq N_g$, which results in

$$\boldsymbol{v}(\hat{\boldsymbol{x}}) \triangleq \boldsymbol{z}(\hat{\boldsymbol{x}}) \odot \boldsymbol{g}(\hat{\boldsymbol{x}}). \tag{36}$$

Multiplicative modification of the SLSHT distribution in spatio-spectral domain is depicted in the first two blocks of Fig. 3(a).

Remark 3: Since each component of the SLSHT distribution describes the contribution of spherical harmonic in the spatial domain, the multiplication of the filter function $\boldsymbol{z}(\hat{\boldsymbol{x}})$ and the SLSHT distribution $\boldsymbol{g}(\hat{\boldsymbol{x}})$ can be thought of as a type of spatially-varying spectral filtering.

Remark 4: If the filter function $\boldsymbol{z}(\hat{\boldsymbol{x}})$ is real, then the kernel $\boldsymbol{\zeta}(\hat{\boldsymbol{x}}, \hat{\boldsymbol{y}})$ in (34) is real and satisfies $\boldsymbol{\zeta}(\hat{\boldsymbol{x}}, \hat{\boldsymbol{y}}) = \boldsymbol{\zeta}(\hat{\boldsymbol{y}}, \hat{\boldsymbol{x}})$, which implies that the operator is self adjoint.

The general least squares approximation method of $\boldsymbol{v}(\hat{\boldsymbol{x}})$ is shown in the third block of Fig. 3(a) according to (29). For the special case of exact recovery, we can explicitly provide the expression for obtaining the signal exactly from the modified distribution $\boldsymbol{v}(\hat{\boldsymbol{x}})$.

Lemma 1: If the MMD, $\boldsymbol{v}(\hat{\boldsymbol{x}})$ given in (36), is a valid SLSHT distribution, then the n-th spherical harmonic coefficient of the transformed signal $d(\hat{\boldsymbol{x}})$, denoted by $(d)_n$, is related to the signal $f(\hat{\boldsymbol{x}})$ as

$$(d)_n = \frac{1}{K} \int_{\mathbb{S}^2} f(\hat{\boldsymbol{x}}) w_n(\hat{\boldsymbol{x}}) \overline{Y_n(\hat{\boldsymbol{x}})}\, ds(\hat{\boldsymbol{x}}), \tag{37}$$

where $w_n(\hat{\boldsymbol{x}})$ is the result of isotropic convolution of the n-th filter component $z(\hat{\boldsymbol{x}}; n)$ and the azimuthally symmetric window function $h(\hat{\boldsymbol{x}})$. That is,

$$w_n(\hat{\boldsymbol{x}}) = \int_{\mathbb{S}^2} \big(\mathcal{D}(\phi, \theta, 0) h\big)(\hat{\boldsymbol{y}})\, z(\hat{\boldsymbol{y}}; n)\, ds(\hat{\boldsymbol{y}}), \quad \hat{\boldsymbol{x}} = \hat{\boldsymbol{x}}(\theta, \phi). \tag{38}$$

Proof: See Appendix C. ■

In what follows, we first explicitly discuss the case where the MMD, $\boldsymbol{v}(\hat{\boldsymbol{x}})$, is a valid SLSHT distribution and provide the elements of the transformation matrix $\boldsymbol{\Upsilon}$ for this special case. We then discuss the elements of the transformation matrix $\boldsymbol{\Upsilon}$ in the general approximation approach.

Lemma 2: Assume that the MMD, $\boldsymbol{v}(\hat{\boldsymbol{x}})$, is a valid SLSHT distribution. Then the spatio-spectral transformation matrix $\boldsymbol{\Upsilon}$ in (31), which relates $\boldsymbol{d}$ to $\boldsymbol{f}$, is given by

$$\boldsymbol{\Upsilon} = \frac{1}{K} \int_{\mathbb{S}^2} \Big\{ \mathrm{diag}\big(\boldsymbol{z}(\hat{\boldsymbol{x}})\big)\, \boldsymbol{\Psi}(\hat{\boldsymbol{x}}) \Big\}_{N_f} ds(\hat{\boldsymbol{x}}), \tag{39}$$

where $\mathrm{diag}\big(\boldsymbol{z}(\hat{\boldsymbol{x}})\big)$ returns the diagonal matrix with diagonal entries specified by $\boldsymbol{z}(\hat{\boldsymbol{x}})$ and $\{\cdot\}_{N_f}$ selects the first sub-matrix of size $(N_f + 1) \times (N_f + 1)$. The entries of $\boldsymbol{\Upsilon}$ are

$$\begin{aligned}\Upsilon_{u,u'} &= \frac{1}{K} \int_{\mathbb{S}^2} z(\hat{\boldsymbol{x}}; u)\, \psi_{u,u'}(\hat{\boldsymbol{x}})\, ds(\hat{\boldsymbol{x}}) \\ &= \sum_{r=0}^{\min(N_h,\, N_{z_u})} \frac{T(u'; r; u)\, (h)_p^0\, (z_u)_r}{(h)_0^0 \sqrt{2p+1}}, \quad (p, q) \leftrightarrow r.\end{aligned} \tag{40}$$

Proof: See Appendix C. ■

Lemma 3: For multiplicative modification of the SLSHT distribution, the general spatio-spectral transformation matrix $\boldsymbol{\Upsilon}$ in (32) is simplified to

$$\boldsymbol{\Upsilon} = \frac{1}{\mathcal{E}} \left(\int_{\mathbb{S}^2} \boldsymbol{\Psi}^H(\hat{\boldsymbol{x}}) \big(\mathrm{diag}\big(\boldsymbol{z}(\hat{\boldsymbol{x}})\big)\, \boldsymbol{\Psi}(\hat{\boldsymbol{x}})\big)\, ds(\hat{\boldsymbol{x}}) \right), \tag{41}$$

with entries given by

$$\begin{aligned}\Upsilon_{u,u'} &= \frac{1}{\mathcal{E}} \sum_{n=0}^{N_g} \sum_{r=0}^{N_h} \sum_{r'=0}^{N_h} \sum_{c=0}^{N_{z_n}} \frac{4\pi}{\sqrt{(2p+1)(2p'+1)}} \\ &\quad \times \overline{(h)_p^0} (h)_{p'}^0 (z_n)_c T(u; r; n)\, T(u'; r'; n)\, T(r; c; r'),\end{aligned} \tag{42}$$

where the mappings $(\ell, m) \leftrightarrow n$, $(p, q) \leftrightarrow r$, $(p', q') \leftrightarrow r'$ and $(s, t) \leftrightarrow u$ are used.

Proof: See Appendix C. ■

We note that this approximate solution cannot be further simplified because of the coupling of Wigner-$3j$ symbols.

B. Convolutive Modification of the SLSHT Distribution

We now consider signal transformation in the spatio-spectral domain as the convolutive modification of the SLSHT distribution, which can be achieved through convolution of the filter function $\boldsymbol{z}(\hat{\boldsymbol{x}})$ and the SLSHT distribution $\boldsymbol{g}(\hat{\boldsymbol{x}})$. The convolutive modification can also be thought of as spatially-varying spectral filtering of the signal, which is accomplished by filtering the spatially-varying spectral components of the signal in spatial domain. The analog of convolutive modification in time-frequency analysis is the smoothing of time-frequency distribution to remove the artifacts in the time-frequency domain [41], [42]. We first specify the kernel $\boldsymbol{\zeta}(\hat{\boldsymbol{x}}, \hat{\boldsymbol{y}})$ in terms of the convolutive filter function and then express this operation as a linear transformation of the signal. Later, we discuss the special case in which each component of the filter function is azimuthally symmetric.

Definition 3 (Convolutive SLSHT Modification): Let $\hat{\boldsymbol{x}} = \hat{\boldsymbol{x}}(\theta,\phi)$ and a spatio-spectral filter function $\boldsymbol{z}(\hat{\boldsymbol{y}})$ be given according to Definition 1. The kernel $\boldsymbol{\zeta}(\hat{\boldsymbol{x}},\hat{\boldsymbol{y}})$ in (21) is obtained by rotating each component of $\boldsymbol{z}(\hat{\boldsymbol{y}})$, such as $z(\hat{\boldsymbol{y}};n)$, as follows

$$\begin{aligned}\boldsymbol{\zeta}(\hat{\boldsymbol{x}},\hat{\boldsymbol{y}}) &\triangleq \big(\mathcal{D}(\phi,\theta,0)\boldsymbol{z}\big)(\hat{\boldsymbol{y}})\\ &= \Big(\big(\mathcal{D}(\phi,\theta,0)z\big)(\hat{\boldsymbol{y}};0),\ \big(\mathcal{D}(\phi,\theta,0)z\big)(\hat{\boldsymbol{y}};1),\\ &\qquad \ldots,\big(\mathcal{D}(\phi,\theta,0)z\big)(\hat{\boldsymbol{y}};N_g)\Big)'. \end{aligned} \tag{43}$$

As a result, the convolutive modified distribution (CMD) $\boldsymbol{v}(\hat{\boldsymbol{x}})$ will have the elements given by

$$\begin{aligned} v(\hat{\boldsymbol{x}};n) &= \int_{\mathbb{S}^2}\big(\mathcal{D}(\phi,\theta,0)z\big)(\hat{\boldsymbol{y}};n)\,g(\hat{\boldsymbol{y}};n)\,ds(\hat{\boldsymbol{y}}),\\ \hat{\boldsymbol{x}} &= \hat{\boldsymbol{x}}(\theta,\phi), \end{aligned}\tag{44}$$

for $0 \le n \le N_g$. More concisely, we can write

$$\boldsymbol{v}(\hat{\boldsymbol{x}}) \triangleq \big(\boldsymbol{z} \circledast \boldsymbol{g}\big)(\hat{\boldsymbol{x}}) \tag{45}$$

where '$\circledast$' denotes spherical convolution operation. This type of filtering in spatio-spectral domain as convolutive modification of the SLSHT distribution is depicted in the first two blocks of Fig. 3(b).

Using the definition of the SLSHT distribution $\boldsymbol{g}(\hat{\boldsymbol{x}})$ for signal $f(\hat{\boldsymbol{x}})$, we now formulate an expression that relates the CMD $\boldsymbol{v}(\hat{\boldsymbol{x}})$ to $\boldsymbol{f} = \big(\mathcal{F}f\big)(\hat{\boldsymbol{x}})$. Such a relation will be useful in finding the signal $d(\hat{\boldsymbol{x}})$ with spectral response $\boldsymbol{d}$ that corresponds to the CMD $\boldsymbol{v}(\hat{\boldsymbol{x}})$, and in expressing $\boldsymbol{d}$ as a linear transformation of $\boldsymbol{f}$. This is accomplished by defining the matrix $\boldsymbol{\Gamma}(\hat{\boldsymbol{x}}) \triangleq \boldsymbol{z}(\hat{\boldsymbol{x}}) \circledast \boldsymbol{\Psi}(\hat{\boldsymbol{x}})$ of size $(N_g+1)\times(N_f+1)$ with entries

$$\begin{aligned}\Gamma_{n,u}(\hat{\boldsymbol{x}}) &= \int_{\mathbb{S}^2}\big(\mathcal{D}(\phi,\theta,0)z\big)(\hat{\boldsymbol{y}};n)\,\psi_{n,u}(\hat{\boldsymbol{y}})\,ds(\hat{\boldsymbol{y}})\\ &= \sum_{r=0}^{\min(N_h,N_{z_n})}\sum_{q'=-p}^{p}\sqrt{\frac{4\pi}{2p+1}}(h)_p^0\,(z_n)_p^{q'}\\ &\quad\times T(u;r;n)\,D_p^{q,q'}(\phi,\theta,0), \end{aligned}\tag{46}$$

with $\hat{\boldsymbol{x}} = \hat{\boldsymbol{x}}(\theta,\phi)$ and $r \leftrightarrow (p,q)$, which is obtained using (13) and (17). Therefore, referring to (16) we express the CMD $\boldsymbol{v}(\hat{\boldsymbol{x}})$ in (45) as

$$\boldsymbol{v}(\hat{\boldsymbol{x}}) = \boldsymbol{\Gamma}(\hat{\boldsymbol{x}})\boldsymbol{f}. \tag{47}$$

Now, we derive the expressions for spatio-spectral transform matrix $\boldsymbol{\Upsilon}$ in (31) for both exact and approximate cases.

Lemma 4: If the CMD $\boldsymbol{v}(\hat{\boldsymbol{x}})$ defined in (45) is a valid SLSHT distribution, the spatio-spectral transform matrix $\boldsymbol{\Upsilon}$ is obtained by using the inversion operation defined in (18) as

$$\boldsymbol{\Upsilon} = \frac{1}{K}\int_{\mathbb{S}^2}\Big\{\boldsymbol{\Gamma}(\hat{\boldsymbol{x}})\Big\}_{N_f} ds(\hat{\boldsymbol{x}}), \tag{48}$$

where entries are obtained by integrating the elements of $\boldsymbol{\Gamma}(\hat{\boldsymbol{x}})$ in (46) as

$$\begin{aligned}\Upsilon_{u,u'} &= \sum_{r=0}^{\min(N_h,N_{z_u})}\sum_{q'=-p}^{p}\frac{1}{(h)_0^0\sqrt{2p+1}}(h)_p^0\,(z_u)_p^{q'}\\ &\quad\times T(u';r,u)\int_{\mathbb{S}^2}D_p^{q,q'}(\phi,\theta,0)\,ds(\hat{\boldsymbol{x}}). \end{aligned}\tag{49}$$

The integral above can be evaluated using the relation between spherical harmonic function and Wigner-D function in (8) and the expression for the integral of associated Legendre function [43] as

$$\int_{\mathbb{S}^2} D_p^{q,q'}(\phi,\theta,0)\,ds(\hat{\boldsymbol{x}}) = 2\pi\,\delta_{q,0}\int_0^{\pi} d_p^{0,q'}(\theta)\sin\theta\,d\theta \tag{50}$$

$$= 2\pi\begin{cases} -\dfrac{2q'\left(\frac{p}{2}\right)!\left(\frac{p}{2}\right)!\sqrt{(p-q')!(p+q')!}}{p\left(\frac{(p+q')}{2}\right)!\left(\frac{(p-q')}{2}\right)!(p+1)!} & \text{if } p \text{ is even, } q' \text{ is even, and } q=0,\\ -\dfrac{q'\pi\,(p+1)!\sqrt{(p-q')!(p+q')!}}{p\,2^{2p+1}\left(\frac{(p+q')}{2}\right)!\left(\frac{(p-q')}{2}\right)!\left(\frac{(p+1)}{2}\right)!} & \text{if } p \text{ is odd, } q' \text{ is odd, and } q=0,\\ 0 & \text{otherwise.}\end{cases} \tag{51}$$

Proof: The proof follows directly from (46) and is omitted for brevity. ■

Lemma 5: For the case that the CMD $\boldsymbol{v}(\hat{\boldsymbol{x}})$ in (45) is not a valid SLSHT distribution, the approximate solution presented in Theorem 1 specializes to

$$\boldsymbol{\Upsilon} = \frac{1}{\mathcal{E}}\int_{\mathbb{S}^2}\boldsymbol{\Psi}^H(\hat{\boldsymbol{x}})\,\boldsymbol{\Gamma}(\hat{\boldsymbol{x}})\,ds(\hat{\boldsymbol{x}}) \tag{52}$$

with entries

$$\begin{aligned}\Upsilon_{u,u'} &= \frac{1}{\mathcal{E}}\sum_{n=0}^{N_g}\int_{\mathbb{S}^2}\overline{\psi_{n,u}(\hat{\boldsymbol{x}})}\Gamma_{n,u'}(\hat{\boldsymbol{x}})\,ds(\hat{\boldsymbol{x}})\\ &= \frac{1}{\mathcal{E}}\sum_{n=0}^{N_g}\sum_{r=0}^{N_h}\sum_{r'=0}^{\min(N_h,N_{z_n})}\sum_{q''=-p'}^{p'}\frac{4\pi}{\sqrt{(2p+1)}}\\ &\quad\times\overline{(h)_p^0}\frac{1}{\sqrt{(2p'+1)}}\overline{(h)_p^0}(h)_{p'}^0\,(z_n)_{p'}^{q''}\,T(u;r;n)\\ &\quad\times T(u';r';n)\int_{\mathbb{S}^2}D_{p'}^{q',q''}(\phi,\theta,0)Y_r(\hat{\boldsymbol{x}})\,ds(\hat{\boldsymbol{x}}), \end{aligned}\tag{53}$$

where the mappings $(p,q) \leftrightarrow r$ and $(p',q') \leftrightarrow r'$ are used. The integral in (53) is the projection of Wigner-D function $D_{p'}^{q',q''}(\phi,\theta,0)$ onto spherical harmonics and can be evaluated by employing the expansion of product of Wigner-D functions using Wigner $3j$ symbols. The details are provided in Appendix D.

Proof: We use (29), (31), and (47) to infer (52). Equation (53) follows from (46) and (75), where the latter is defined in Appendix D. ■

Again, further simplification of this approximate solution is not possible because of coupling of Wigner-$3j$ symbols and irreducible Wigner-D functions. However, for the special case where each component of the filter function is azimuthally symmetric, we obtain further simplifications as follows.

1) Special Case – Azimuthally Symmetric Filter Function: If each component of the filter function is azimuthally symmetric, then $(z_n)_{p'}^{q''} = 0$ for $q'' \neq 0$ in (53) for all $n \in [0, N_g]$. Using the relation between Wigner-D function and spherical harmonic in (8) and orthonormal property of spherical harmonics, the expression for the entries $\Upsilon_{u,u'}$ in (53) simplifies to

$$\begin{aligned}\Upsilon_{u,u'} &= \frac{1}{\mathcal{E}}\sum_{n=0}^{N_g}\sum_{r=0}^{\min(N_h,N_{z_n})}\left(\frac{4\pi}{2p+1}\right)^{\frac{3}{2}}\left|(h)_p^0\right|^2\\ &\quad\times(z_n)_p^0\,T(u;r;n)\,T(u';r;n), \qquad (p,q)\leftrightarrow r \end{aligned}\tag{54}$$

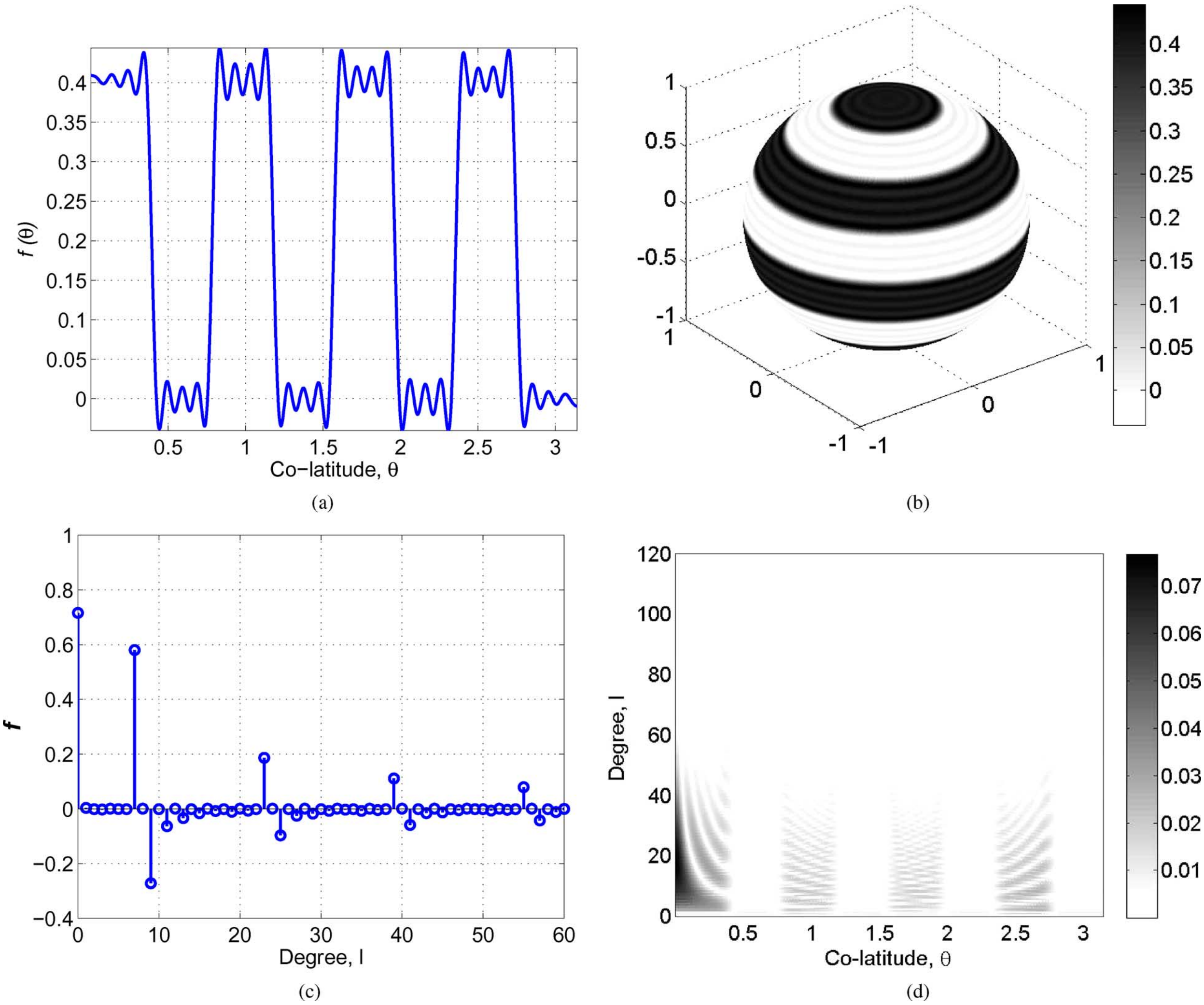

Fig. 4. Signal $f(\hat{\boldsymbol{x}}) = f(\theta)$: (a) as a function of co-latitude θ and (b) on the sphere. (c) Spectrum of the signal $\boldsymbol{f}$ vs degree ℓ for order $m = 0$, $(f)_\ell^0$. (d) SLSHT distribution $\boldsymbol{g}(\hat{\boldsymbol{x}})$ of the signal as a function of degree ℓ and co-latitude θ.

Let us assume that in addition to being azimuthally symmetric, the components of filter function also satisfy $z(\hat{\boldsymbol{x}};n) = z(\hat{\boldsymbol{x}};\ell)$ with the mapping $(\ell,m) \leftrightarrow n$ for all $n \in [0, N_g]$, which indicates that there is the same filter function component of degree ℓ for all the spherical harmonic orders $-\ell \le m \le \ell$. With this assumption and employing the orthogonality relations of Wigner-$3j$ symbols [17], $\Upsilon_{u,u'}$ in (54) simplifies to

$$\Upsilon_{u,u'} = \frac{1}{\mathcal{E}} \sum_{\ell=0}^{L_g} \sum_{p=0}^{\min(L_h, L_{z_n})} (2\ell+1)\sqrt{\frac{4\pi}{2p+1}} \times (z_\ell)_p^0 \left|(h)_p^0\right|^2 \begin{pmatrix} s & p & \ell \\ 0 & 0 & 0 \end{pmatrix}^2 \delta_{u,u'} \quad (55)$$

and the spatio-spectral transformation matrix $\boldsymbol{\Upsilon}$ becomes a diagonal matrix.

V. Examples

In this section, we provide an illustration of the filtering operation in spatio-spectral domain. In our experiments, we have implemented the method outlined in [8] to calculate the spherical harmonic coefficients and the triple product (15) in MATLAB. We use equiangular sampling with $M \times M$ samples on the sphere as $\theta_m = \frac{\pi m}{M}$, $\phi_m = \frac{2\pi m}{M}$ for $m = 0, 1, \ldots, M-1$. Note that the exact quadrature can be evaluated using this tessellation. We use the most optimally concentrated azimuthally symmetric bandlimited Slepian eigenfunction as the window function to obtain the SLSHT distribution of a signal [1], [15]. For inverse spherical harmonic transform of a function with the maximum spherical harmonic degree L, we use the minimum resolution $M = 2(L+1)$ for the evaluation of exact quadrature [8]. Furthermore, we consider unit energy normalized functions in our experiments.

A. First Example

In our first example, we consider the bandlimited azimuthally symmetric signal $f(\hat{\boldsymbol{x}}) = f(\theta)$ on the sphere with the maximum spherical harmonic degree $L_f = 60$. The signal under consideration is shown in Fig. 4(a) and (b) and is obtained by spectrally truncating the following signal $f_1(\hat{\boldsymbol{x}})$ defined as

$$f_1(\hat{\boldsymbol{x}}) = f_1(\theta) \triangleq \begin{cases} 1 & \theta \in \left[0, \frac{\pi}{8}\right] \cup \left[\frac{\pi}{4}, \frac{3\pi}{8}\right] \cup \left[\frac{\pi}{2}, \frac{5\pi}{8}\right] \cup \left[\frac{3\pi}{4}, \frac{7\pi}{8}\right] \\ 0 & \text{otherwise,} \end{cases} \quad (56)$$

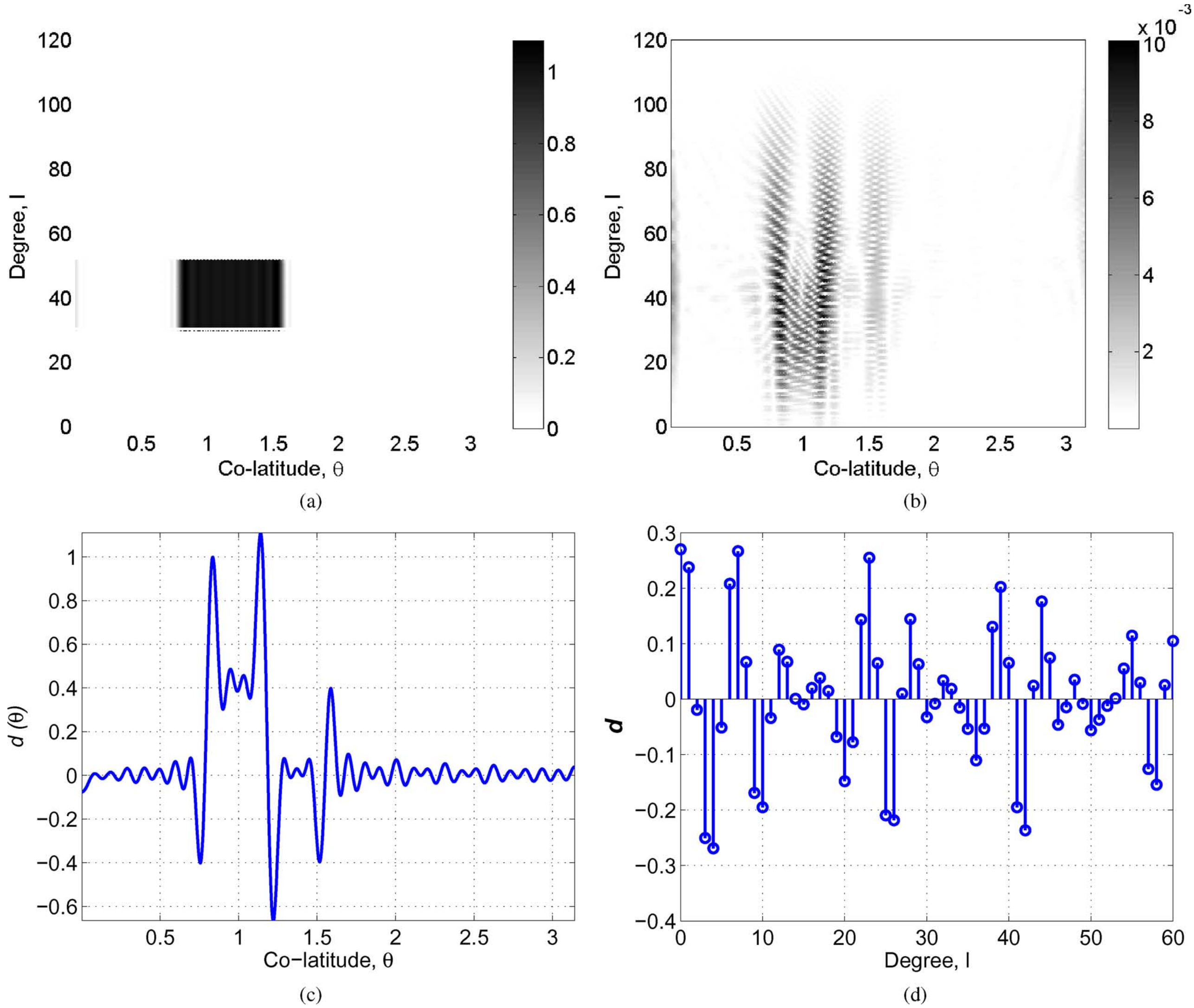

Fig. 5. (a) Spatially-varying filter $z(\hat{\boldsymbol{x}})$ as defined in (57). (b) The approximated distribution $\hat{\boldsymbol{v}}(\hat{\boldsymbol{x}})$ as the SLSHT distribution of the signal $d(\hat{\boldsymbol{x}})$. (c) Signal $d(\hat{\boldsymbol{x}}) = d(\theta)$ in spatial domain as a function of co-latitude θ and (d) in spectral domain as $\boldsymbol{d}$ vs degree ℓ for order $m = 0$.

to a maximum spherical harmonic degree L_f. Since the signal is azimuthally symmetric, only zero-order spherical harmonic coefficients $(f)_\ell^0$ can be non-zero, which are shown in Fig. 4(c). Since we are seeking the contribution of zero-order spherical harmonics, the SLSHT distribution $\boldsymbol{g}(\hat{\boldsymbol{x}})$ is shown in Fig. 4(d) as a function of co-latitude θ and degree ℓ. The SLSHT distribution is obtained using an azimuthally symmetric eigenfunction window of maximum degree $L_h = 60$, which is spatially concentrated in the region $0 \leq \theta \leq \frac{\pi}{30}$. We are interested to obtain the MMD $\boldsymbol{v}(\hat{\boldsymbol{x}})$, defined in (36), using the following filter function $\boldsymbol{z}(\hat{\boldsymbol{x}})$

$$z(\hat{\boldsymbol{x}}; \ell, 0) = \begin{cases} 1 & 30 \leq \ell \leq 50,\ \frac{\pi}{4} \leq \theta \leq \frac{\pi}{2}, 0 \leq \phi < 2\pi \\ 0 & \text{otherwise} \end{cases} \tag{57}$$

where the maximum spectral degree is considered to be $L_{z_n} = 60$ for each non-zero filter component $z(\hat{\boldsymbol{x}}; \ell, 0)$ for $30 \leq \ell \leq 50$. The filter function $\boldsymbol{z}(\hat{\boldsymbol{x}})$ is shown in spatio-spectral domain in Fig. 5(a) as a function of degree ℓ and co-latitude θ. The negligible ringing, which can be observed outside the spatio-spectral region defined in (57) along the spatial domain, is due to the consideration that each component of filter function is bandlimited with $L_{z_n} = 60$. Since the filter function truncates $\boldsymbol{g}(\hat{\boldsymbol{x}})$ both in the spatial and spectral domain, the resulting MMD $\boldsymbol{v}(\hat{\boldsymbol{x}})$ is not a valid SLSHT distribution. Therefore, we employ the approximate solution to determine the signal $d(\hat{\boldsymbol{x}}) = d(\theta)$, the SLSHT distribution of which best approximates the MMD $\boldsymbol{v}(\hat{\boldsymbol{x}})$ in least squares sense. The approximated distribution $\hat{\boldsymbol{v}}(\hat{\boldsymbol{x}})$ is shown in Fig. 5(b) which is the SLSHT distribution of signal $d(\hat{\boldsymbol{x}})$. The signal $d(\hat{\boldsymbol{x}})$ is shown in Fig. 5(c) and (d) in the spatial and spectral domains, respectively. The approximated distribution $\hat{\boldsymbol{v}}(\hat{\boldsymbol{x}})$ shows that the signal is concentrated around the desired spatio-spectral region. There are some artifacts near the poles at $\theta = 0$ and $\theta = \pi$, which is due to the fact that zero-order spherical harmonics have relatively higher values near the poles.

B. Second Example

The type of filtering shown in Section V-A which truncates the signal in spatio-spectral domain can also be considered as spatial truncation followed by spectral truncation. However, this

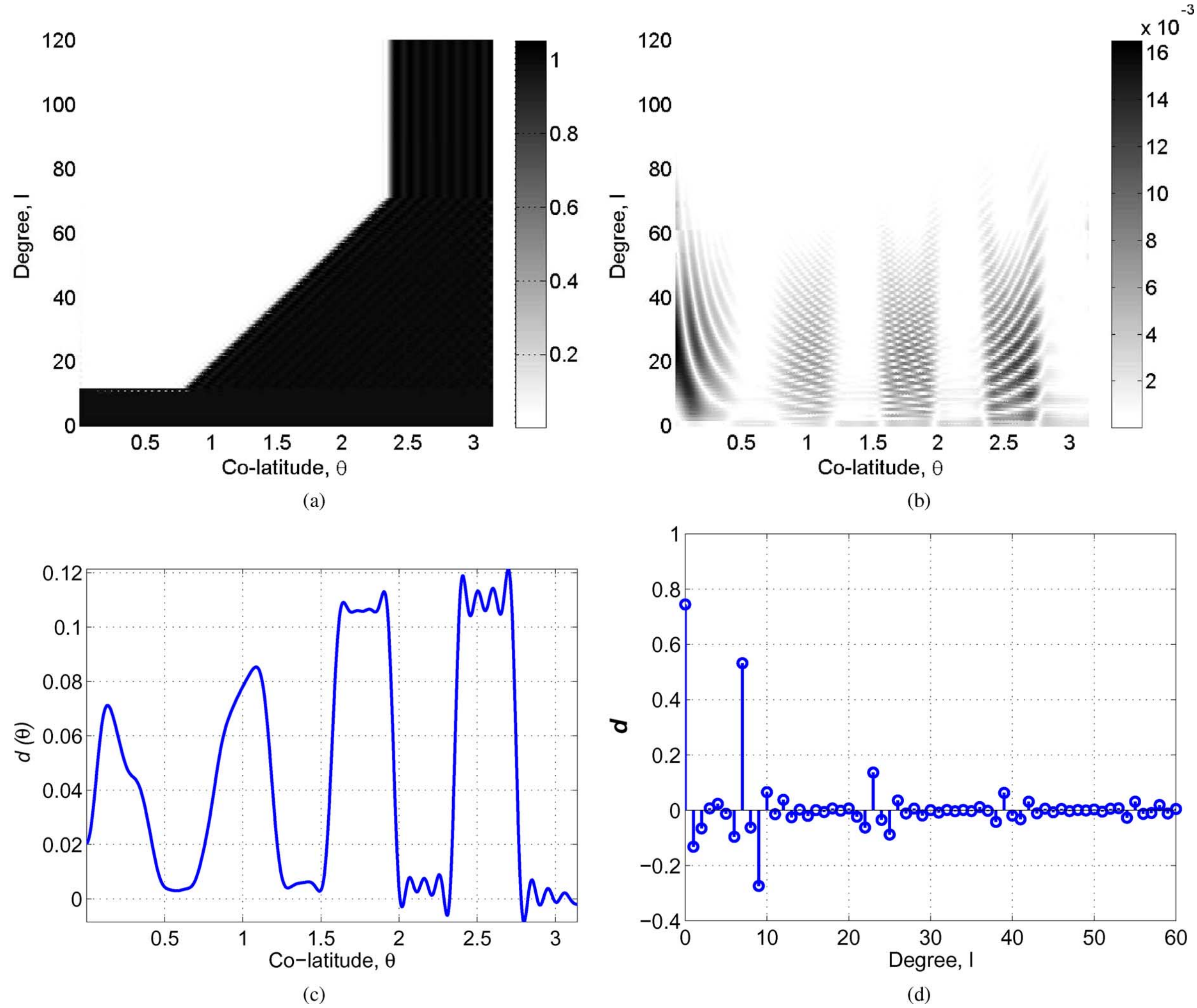

Fig. 6. (a) Spatially-varying filter $z(\hat{\boldsymbol{x}})$ as defined in (58). (b) The approximated distribution $\hat{\boldsymbol{v}}(\hat{\boldsymbol{x}})$ as the SLSHT distribution of the signal $d(\hat{\boldsymbol{x}})$. (c) Signal $d(\hat{\boldsymbol{x}}) = d(\theta)$ in spatial domain as a function of co-latitude θ and (d) in spectral domain as $\boldsymbol{d}$ vs degree ℓ for order $m = 0$.

will not ensure the concentration of the filtered signal in the spatio-spectral domain. In order to further illustrate the capability of the proposed framework, we consider another example of multiplicative modification of the SLSHT distribution, in which we carry out spatially-varying spectral filtering in the spatio-spectral domain.

We consider the following filter function $z(\hat{\boldsymbol{x}})$ in the spatio-spectral domain

$$z(\hat{\boldsymbol{x}};\ell,0)=\begin{cases}1 & 0\le\ell\le 10, 0\le\theta\le\pi, 0\le\phi<2\pi\\ 1 & 11\le\ell\le 70, \frac{(\ell+20)\pi}{120}\le\theta\le\pi, 0\le\phi<2\pi\\ 1 & 71\le\ell\le 120, \frac{3\pi}{4}\le\theta\le\pi, 0\le\phi<2\pi,\\ 0 & \text{otherwise},\end{cases} \tag{58}$$

which is shown in Fig. 6(a), where we have again assumed that each filter function component is bandlimited with the maximum spherical harmonic degree equal to $L_{z_n} = 60$. It is evident from the Fig. 6(a) that the filter function is spatially-varying in the spatio-spectral domain and thus filters out different spectral contents in different spatial regions. For example, it filters the contribution of all spherical harmonics of degree greater than 10 around $\theta = \frac{\pi}{4}$ region, whereas it filters spherical harmonics of degree greater than 70 around $\theta = \frac{3\pi}{4}$ region. Thus such type of filtering can be regarded as spatially-varying low pass filtering, where the bandwidth of the filter function is changing with the co-latitude. Using proposed least squares solution, we determine the signal $d(\hat{\boldsymbol{x}})$ whose SLSHT distribution approximates the MMD $\boldsymbol{v}(\hat{\boldsymbol{x}})$ in least squares sense. The approximated distribution $\hat{\boldsymbol{v}}(\hat{\boldsymbol{x}})$ in spatio-spectral domain and the signal $d(\hat{\boldsymbol{x}})$ in spatial and spectral domains are shown in Fig. 6(b)–(d), where the effect of spatially-varying low-pass filtering is apparent.

VI. Conclusion

The spatially localized spherical harmonic transform (SLSHT) distribution presents a mechanism to transform, modify and filter the signal in the joint spatio-spectral domain to realize spatially varying spectral filtering. As in the time-frequency analogy, such a transformation in the spatio-spectral domain can lead to a modified distribution that is not a SLSHT distribution of physically valid spatial signal. Therefore, we formulated and solved an optimization problem to find the closest physically valid signal to the modified SLHT distribution by deriving an expression for an appropriate inverse spatio-spectral transform.

We illustrated two types of transformation to the SLSHT distribution, both being instances of a general linear integral operator. Multiplicative modification of the SLSHT was considered in Section IV-B and a convolutive modification was considered in Section IV-C. Both can be regarded as representing spatially varying spectral filtering. The power of the technique was illustrated in two examples of spatially-varying spectral that allows processing of signals in joint spatio-spectral domain, in a way that cannot be accomplished separately in either spatial or spectral domain.

There are natural generalizations of the work presented. The technique we developed to recover a spectral response of a valid signal on the unit sphere from a modified SLSHT distribution is not limited to linear transformations in the spatio-spectral domain. Since there exist efficient computational techniques to *exactly* evaluate the spherical harmonic transform of the bandlimited signals [8], [18], we have considered the signal in the spectral domain in the proposed mathematical developments and formulations. We consider the development of efficient computational techniques to do the given processing as an open problem for further work.

Appendix A
Mathematical Background

Spherical Harmonics: The spherical harmonic function, $Y_\ell^m(\hat{\boldsymbol{x}}) = Y_\ell^m(\theta,\phi)$, for degree $\ell \geq 0$ and order $|m| \leq \ell$ is defined as [17]

$$Y_\ell^m(\theta,\phi) = N_\ell^m P_\ell^m(\cos\theta)\, e^{im\phi}, \tag{59}$$

where N_ℓ^m is the normalization factor given by

$$N_\ell^m \triangleq \sqrt{\frac{2\ell+1}{4\pi}\frac{(\ell-m)!}{(\ell+m)!}}, \tag{60}$$

such that $\langle Y_\ell^m, Y_p^q\rangle = \delta_{\ell,p}\delta_{m,q}$, where $\delta_{m,q}$ is the Kronecker delta function: $\delta_{m,q} = 1$ for $m = q$ and is zero otherwise. $P_\ell^m(x)$ is the associated Legendre function defined for degree ℓ and order $0 \leq m \leq \ell$ as

$$P_\ell^m(x) = \frac{(-1)^m}{2^\ell \ell!}(1-x^2)^{\frac{m}{2}}\frac{d^{\ell+m}}{dx^{\ell+m}}(x^2-1)^\ell$$
$$P_\ell^{-m}(x) = (-1)^m\frac{(\ell-m)!}{(\ell+m)!}P_\ell^m(x),$$

for $|x| \leq 1$. We also note the following relation between $Y_\ell^m(\hat{\boldsymbol{x}})$ and $Y_\ell^{-m}(\hat{\boldsymbol{x}})$

$$\overline{Y_\ell^m(\hat{\boldsymbol{x}})} = (-1)^m Y_\ell^{-m}(\hat{\boldsymbol{x}}). \tag{61}$$

Spherical Dirac Delta Function: The Dirac delta function $\delta(\hat{\boldsymbol{x}},\hat{\boldsymbol{y}})$ on the sphere with the sifting property

$$f(\hat{\boldsymbol{x}}) = \int_{\mathbb{S}^2}\delta(\hat{\boldsymbol{x}},\hat{\boldsymbol{y}})f(\hat{\boldsymbol{y}})\,ds(\hat{\boldsymbol{y}}), \tag{62}$$

has following expansion, called the completeness relation, in spherical harmonic domain

$$\delta(\hat{\boldsymbol{x}},\hat{\boldsymbol{y}}) = \sum_{\ell=0}^{\infty}\sum_{m=-\ell}^{\ell} Y_\ell^m(\hat{\boldsymbol{x}})\overline{Y_\ell^m(\hat{\boldsymbol{y}})}. \tag{63}$$

Note that $\delta(\hat{\boldsymbol{x}},\hat{\boldsymbol{y}}) \notin L^2(\mathbb{S}^2)$.

Spherical Harmonics Triple Product: Using the Wigner-$3j$ symbols [17], the spherical harmonic triple product $T(u;r;n)$ can be written using the mappings $(s,t) \leftrightarrow u$, $(p,q) \leftrightarrow r$ and $(\ell,m) \leftrightarrow n$ as

$$T(u;r;n) = (-1)^m\sqrt{\frac{(2s+1)(2p+1)(2\ell+1)}{4\pi}} \times \begin{pmatrix} s & p & \ell \\ 0 & 0 & 0 \end{pmatrix}\begin{pmatrix} s & p & \ell \\ t & q & -m \end{pmatrix}. \tag{64}$$

We note that Wigner-$3j$ symbols [17] are real-valued. Therefore, $\overline{T(u;r;n)} = T(u;r;n)$, which can also be directly proven using (15), symmetry relations of Wigner-$3j$ symbols and the fact that $T(u;r;n)$ is non-zero only when $s+p+\ell$ is even.

Wigner-d Functions: The Wigner-d function $d_\ell^{m,m'}(\theta)$ used in (6) is defined as [17], [44]

$$d_\ell^{m,m'}(\theta) = \sum_j (-1)^{j-m'+m} \times \frac{\sqrt{(\ell+m')!(\ell-m')!(\ell+m)!(\ell-m)!}}{(\ell+m'-j)!(j)!(\ell-j-m)!(j-m'+m)!} \times \cos\left(\frac{\theta}{2}\right)^{2\ell-2j+m'-m}\sin\left(\frac{\theta}{2}\right)^{2j-m'+m}, \tag{65}$$

where the sum is over all j such that denominator terms do not become negative.

Appendix B
Proof of Theorem 1 (Least Squares Solution)

We take the derivative of the total error E in (27) with respect to the u-th element of $\boldsymbol{d}$, $(d)_u$, and set it to zero

$$\frac{\partial E}{\partial (d)_u} = \int_{\mathbb{S}^2}\sum_{n=0}^{N_g}\frac{\partial\left|e(\hat{\boldsymbol{x}};n)\right|^2}{\partial (d)_u}\,ds(\hat{\boldsymbol{x}}) = 0.$$

Now using $e(\hat{\boldsymbol{x}};n) \triangleq v(\hat{\boldsymbol{x}};n) - \Psi_{n,:}(\hat{\boldsymbol{x}})\boldsymbol{d} = v(\hat{\boldsymbol{x}};n) - \sum_{u=0}^{N_f}\Psi_{n,u}(\hat{\boldsymbol{x}})(d)_u$ and rearranging the terms results in

$$\int_{\mathbb{S}^2}\sum_{n=0}^{N_g}\sum_{u'=0}^{N_f}\overline{\Psi_{n,u}(\hat{\boldsymbol{x}})}\Psi_{n,u'}(\hat{\boldsymbol{x}})(d)_{u'}\,ds(\hat{\boldsymbol{x}}) = \int_{\mathbb{S}^2}\sum_{n=0}^{N_g}\overline{\Psi_{n,u}(\hat{\boldsymbol{x}})}v(\hat{\boldsymbol{x}};n)\,ds(\hat{\boldsymbol{x}}),$$

which can be written in matrix form as

$$\underbrace{\left(\int_{\mathbb{S}^2} \boldsymbol{\Psi}^H(\hat{\boldsymbol{x}})\,\boldsymbol{\Psi}(\hat{\boldsymbol{x}})\,ds(\hat{\boldsymbol{x}})\right)}_{\boldsymbol{\mathcal{M}}}\boldsymbol{d} = \int_{\mathbb{S}^2} \boldsymbol{\Psi}^H(\hat{\boldsymbol{x}})\boldsymbol{v}(\hat{\boldsymbol{x}})\,ds(\hat{\boldsymbol{x}}), \quad (66)$$

from which (29) becomes clear. Now, let us examine the entries of $\boldsymbol{\mathcal{M}}$ in more detail

$$\mathcal{M}_{u,u'} = \sum_{n=0}^{N_g} \int_{\mathbb{S}^2} \overline{\psi_{n,u}(\hat{\boldsymbol{x}})}\,\psi_{n,u'}(\hat{\boldsymbol{x}})\,ds(\hat{\boldsymbol{x}}). \quad (67)$$

Upon using the definition of the elements of $\boldsymbol{\Psi}$ in (17), we obtain

$$\mathcal{M}_{u,u'} = \sum_{n=0}^{N_g}\sum_{r=0}^{N_h}\sum_{r'=0}^{N_h} \overline{T(u;r;n)}\,T(u';r';n) \times \int_{\mathbb{S}^2} \overline{(h)_r(\hat{\boldsymbol{x}})}(h)_{r'}(\hat{\boldsymbol{x}})\,ds(\hat{\boldsymbol{x}}),$$

which can be simplified using (7) and employing the orthonormal property of spherical harmonics

$$\mathcal{M}_{u,u'} = \sum_{n=0}^{N_g}\sum_{p=0}^{L_h}\sum_{q=-p}^{p} \frac{4\pi}{2p+1}\left|(h)_p^0\right|^2 \overline{T(u;r;n)}\,T(u';r;n),$$

where the mapping $(p,q) \leftrightarrow r$ has been used. Now using $\overline{T(u;r;n)} = T(u;r;n)$, the additional mapping $(s',t') \leftrightarrow u'$ and (64) we arrive at

$$\mathcal{M}_{u,u'} = \sum_{\ell=0}^{L_g}\sum_{p=0}^{L_h}(2\ell+1)\sqrt{(2s+1)(2s'+1)}\left|(h)_p^0\right|^2 \times \begin{pmatrix} s & p & \ell \\ 0 & 0 & 0 \end{pmatrix}\begin{pmatrix} s' & p & \ell \\ 0 & 0 & 0 \end{pmatrix} \times \sum_{m=-\ell}^{\ell}\sum_{q=-p}^{p}(-1)^t(-1)^q(-1)^m \begin{pmatrix} s & p & \ell \\ t & q & -m \end{pmatrix}\begin{pmatrix} s' & p & \ell \\ t' & q & -m \end{pmatrix}.$$

Now we invoke the following orthogonality relation of Wigner-$3j$ symbols,

$$(2s+1)\sum_{m=-\ell}^{\ell}\sum_{q=-p}^{p}\begin{pmatrix} s & p & \ell \\ t & q & -m \end{pmatrix}\begin{pmatrix} s' & p & \ell \\ t' & q & -m \end{pmatrix} = \delta_{s,s'}\,\delta_{t,t'}, \quad (68)$$

to reach that $\mathcal{M}_{u,u'}$ is only non-zero when $s = s'$ and $t = t'$ or when $u = u'$, that is,

$$\mathcal{M}_{u,u} = \sum_{\ell=0}^{L_g}\sum_{p=0}^{L_h}(2\ell+1)\left|(h)_p^0\right|^2\begin{pmatrix} s & p & \ell \\ 0 & 0 & 0 \end{pmatrix}^2 = \sum_{p=0}^{L_h}\left|(h)_p^0\right|^2, \quad (69)$$

where the following identity of Wigner-$3j$ symbols is employed in obtaining the second equality

$$\sum_{\ell=0}^{L_g}(2\ell+1)\begin{pmatrix} s & p & \ell \\ 0 & 0 & 0 \end{pmatrix}^2 = 1, \quad 0 \le p \le L_h,\ 0 \le s \le L_f. \quad (70)$$

We note here that the entries of the matrix $\boldsymbol{\mathcal{M}}$ given by (69) also appeared in [15], [45] as the sum of the rows of the coupling matrix (see [45] for details). With the entries of matrix $\boldsymbol{\mathcal{M}}$ in (69), the $\boldsymbol{\mathcal{M}}$ becomes identity matrix scaled by the energy of the window function defined in (30) and Theorem 1 is proved. ■

Appendix C
Proof of Lemmas 1–3

From the definition of MMD in (35) and using the inversion relation in (18), we conclude that the n-th component of $\boldsymbol{d}$ can be obtained as

$$(d)_n = \frac{1}{\sqrt{4\pi}(h)_0^0}\int_{\mathbb{S}^2} g(\hat{\boldsymbol{x}};n)\,z(\hat{\boldsymbol{x}};n)\,ds(\hat{\boldsymbol{x}}).$$

Using the spherical harmonic expansion $z(\hat{\boldsymbol{x}};n) = \sum_{c=0}^{N_{z_n}}(z_n)_c Y_c(\hat{\boldsymbol{x}})$, the SLSHT distribution formulation in (14) and the orthogonality relation of spherical harmonics, we obtain

$$(d)_n = \frac{1}{\sqrt{4\pi}(h)_0^0}\sum_{u=0}^{N_f}(f)_u \sum_{r=0}^{\min(N_h,N_{z_n})}\sqrt{\frac{4\pi}{2p+1}} \times (h)_p^0\,(z_n)_r\,T(u;r;n), \quad (p,q) \leftrightarrow r. \quad (71)$$

Now according to (10),

$$(w_n)_r \triangleq \sqrt{\frac{4\pi}{2p+1}}\,(h)_p^0\,(z_n)_r, \quad (p,q) \leftrightarrow r \quad (72)$$

can be understood as the spherical harmonic coefficient of the convolution output between $z(\hat{\boldsymbol{x}};n)$ and the azimuthally symmetric window function $h(\hat{\boldsymbol{x}})$. Hence, we can express $(d)_n$ in (71) as

$$(d)_n = \frac{1}{\sqrt{4\pi}(h)_0}\sum_{u=0}^{N_f}(f)_u \sum_{r=0}^{\min(N_h,N_{z_n})}(w_n)_r\,T(u;r;n). \quad (73)$$

Now using the expression for $T(u;r;n)$ on the right hand side of (15), $f(\hat{\boldsymbol{x}}) = \sum_{u=0}^{N_f}(f)_u Y_u(\hat{\boldsymbol{x}})$, and $w_n(\hat{\boldsymbol{x}}) = \sum_{u=0}^{N_f}(w_n)_r Y_r(\hat{\boldsymbol{x}})$ we obtain the stated result in Lemma 1.

Proof of Lemma 2 is easy. First, according to (36) and (16)

$$\boldsymbol{v}(\hat{\boldsymbol{x}}) = \boldsymbol{z}(\hat{\boldsymbol{x}}) \odot \boldsymbol{g}(\hat{\boldsymbol{x}}) = \boldsymbol{z}(\hat{\boldsymbol{x}}) \odot \left(\boldsymbol{\Psi}(\hat{\boldsymbol{x}})\boldsymbol{f}\right) = \left(\operatorname{diag}\left(\boldsymbol{z}(\hat{\boldsymbol{x}})\right)\boldsymbol{\Psi}(\hat{\boldsymbol{x}})\right)\boldsymbol{f}. \quad (74)$$

Therefore, according to (19) we can write the spectral response of signal $d(\hat{\boldsymbol{x}})$, $\boldsymbol{d}$, corresponding to $\boldsymbol{v}(\hat{\boldsymbol{x}})$ as

$$\boldsymbol{d} = \frac{1}{K}\int_{\mathbb{S}^2}\boldsymbol{v}(\hat{\boldsymbol{x}})\,ds(\hat{\boldsymbol{x}}) = \left(\frac{1}{K}\int_{\mathbb{S}^2}\left(\operatorname{diag}\left(\boldsymbol{z}(\hat{\boldsymbol{x}})\right)\boldsymbol{\Psi}(\hat{\boldsymbol{x}})\right)ds(\hat{\boldsymbol{x}})\right)f.$$

And by comparison with (31) we conclude (39).

Equation (40) follows from using (13), (17), $z(\hat{\boldsymbol{x}};u) = \sum_{c=0}^{N_{z_u}}(z_u)_c Y_c(\hat{\boldsymbol{x}})$, and orthogonality relation of spherical harmonics. This was also implied in (72) and (73) in the proof of Lemma 1.

For the proof of Lemma 3, we first use (34) in (32) and the the sifting property of Dirac delta function to arrive at (41). For obtaining the entries of $\boldsymbol{\Upsilon}$, we proceed as follows. From (13) and (17), we know that

$$\psi^H_{u,n}(\hat{\boldsymbol{x}}) = \overline{\psi_{n,u}(\hat{\boldsymbol{x}})} = \sum_{r=0}^{N_h} \sqrt{\frac{4\pi}{2p+1}} Y_r(\hat{\boldsymbol{x}}) \overline{(h)^0_p}\, \overline{T(u;r;n)}, \quad (p,q) \leftrightarrow r, \tag{75}$$

$$\psi_{n,u'}(\hat{\boldsymbol{x}}) = \sum_{r'=0}^{N_h} \sqrt{\frac{4\pi}{2p'+1}} \overline{Y_{r'}(\hat{\boldsymbol{x}})} (h)^0_{p'} T(u';r';n), \quad (p',q') \leftrightarrow r'. \tag{76}$$

Upon using the above, $z(\hat{\boldsymbol{x}};n) = \sum_{c=0}^{N_{z_n}} (z_n)_c Y_c(\hat{\boldsymbol{x}})$ in (41), we obtain

$$\Upsilon_{u,u'} = \frac{1}{\mathcal{E}} \sum_{n=0}^{N_g} \sum_{r=0}^{N_h} \sum_{r'=0}^{N_h} \sum_{c=0}^{N_{z_n}} \frac{4\pi}{\sqrt{(2p+1)(2p'+1)}} \times \overline{(h)^0_p T(u;r;n)}\, T(u';r';n) (h)^0_{p'} (z_n)_c \times \int_{\mathbb{S}^2} Y_r(\hat{\boldsymbol{x}}) Y_c(\hat{\boldsymbol{x}}) \overline{Y_{r'}(\hat{\boldsymbol{x}})}\, ds(\hat{\boldsymbol{x}}). \tag{77}$$

Finally, recalling $\overline{T(u;r;n)} = T(u;r;n)$ and the definition (15) for the integral in (77), we obtain

$$\Upsilon_{u,u'} = \frac{1}{\mathcal{E}} \sum_{n=0}^{N_g} \sum_{r=0}^{N_h} \sum_{r'=0}^{N_h} \sum_{c=0}^{N_{z_n}} \frac{4\pi}{\sqrt{(2p+1)(2p'+1)}} \times \overline{(h)^0_p} (h)^0_{p'} (z_n)_c T(u;r;n)\, T(u';r';n)\, T(r;c;r'), \tag{78}$$

which is identical to (42).

Appendix D
Evaluation of Integral in (53)

Following the relation between Wigner-D function and spherical harmonics in (8), the integral in (53) can be expressed as

$$\int_{\mathbb{S}^2} D^{q',q''}_{p'}(\phi,\theta,0) Y^q_p(\hat{\boldsymbol{x}})\, ds(\hat{\boldsymbol{x}}) = \sqrt{\frac{4\pi}{2p+1}} \int_0^\pi d^{q',q''}_{p'}(\theta) d^{q,0}_p(\theta) \sin\theta d\theta \int_0^{2\pi} e^{-i(q-q')\phi} d\phi = \delta_{q,q'} 2\pi \sqrt{\frac{4\pi}{2p+1}} \int_0^\pi d^{q',q''}_{p'}(\theta) d^{q',0}_p(\theta) \sin\theta d\theta, \tag{79}$$

where the integral over θ can be evaluated by employing the following expansion of product of Wigner-d functions in terms of Wigner-$3j$ symbols and then using the computation of integral given in (50)

$$d^{q',q''}_{p'}(\theta) d^{q',0}_p(\theta) = (-1)^{p+q''-q'} \sum_{c=|p'-p|}^{p'+p} (2c+1)\, d^{0,q''}_c(\theta) \times \begin{pmatrix} p' & p & c \\ q' & -q' & 0 \end{pmatrix} \begin{pmatrix} p' & p & c \\ q'' & 0 & -q'' \end{pmatrix}. \tag{80}$$

References

[1] F. J. Simons, F. A. Dahlen, and M. A. Wieczorek, "Spatiospectral concentration on a sphere," *SIAM Rev.*, vol. 48, no. 3, pp. 504–536, 2006.
[2] D. N. Spergel *et al.*, "Three-year Wilkinson microwave anisotropy probe (WMAP) observations: Implications for cosmology," *Astrophys. J. Suppl. Ser.*, vol. 170, no. 2, pp. 377–408, 2007.
[3] C. Han, B. Sun, R. Ramamoorthi, and E. Grinspun, "Frequency domain normal map filtering," *ACM Trans. Graph.*, vol. 26, no. 3, pp. 28:1–28:12, Jul. 2007.
[4] D. Colton and R. Kress, *Inverse Acoustic and Electromagnetic Scattering Theory*, 2nd ed. Berlin, Germany: Springer-Verlag, 1998.
[5] B. T. T. Yeo, W. Ou, and P. Golland, "On the construction of invertible filter banks on the 2-sphere," *IEEE Trans. Image Process.*, vol. 17, no. 3, pp. 283–300, Mar. 2008.
[6] D. B. Ward, R. A. Kennedy, and R. C. Williamson, "Theory and design of broadband sensor arrays with frequency invariant far-field beam patterns," *J. Acoust. Soc. Am.*, vol. 97, no. 2, pp. 1023–1034, Feb. 1995.
[7] T. S. Pollock, T. D. Abhayapala, and R. A. Kennedy, "Introducing space into MIMO capacity calculations," *J. Telecommun. Syst.*, vol. 24, no. 2, pp. 415–436, Oct. 2003.
[8] J. R. Driscoll and D. M. Healy Jr., "Computing Fourier transforms and convolutions on the 2-sphere," *Adv. Appl. Math.*, vol. 15, no. 2, pp. 202–250, Jun. 1994.
[9] R. A. Kennedy, T. A. Lamahewa, and L. Wei, "On azimuthally symmetric 2-sphere convolution," *Dig. Sig. Process.*, vol. 5, no. 11, pp. 660–666, Sep. 2011.
[10] P. Sadeghi, R. A. Kennedy, and Z. Khalid, "Commutative anisotropic convolution on the 2-sphere," *IEEE Trans. Signal Process.*, 2012, unpublished.
[11] Z. Khalid, S. Durrani, R. A. Kennedy, and P. Sadeghi, "On the construction of low-pass filters on the unit sphere," in *Proc. IEEE Int. Conf. Acoust., Speech, Signal Process. (ICASSP)*, Prague, Czech Republic, May 2011, pp. 4356–4359.
[12] J. McEwen, M. Hobson, and A. Lasenby, "Optimal filters on the sphere," *IEEE Trans. Signal Process.*, vol. 56, no. 8, pp. 3813–3823, Aug. 2008.
[13] J. D. McEwen, M. P. Hobson, D. J. Mortlock, and A. N. Lasenby, "Fast directional continuous spherical wavelet transform algorithms," *IEEE Trans. Signal Process.*, vol. 55, no. 2, pp. 520–529, Feb. 2007.
[14] P. Audet, "Directional wavelet analysis on the sphere: Application to gravity and topography of the terrestrial planets," *J. Geophys. Res.*, vol. 116, Feb. 2011.
[15] M. A. Wieczorek and F. J. Simons, "Localized spectral analysis on the sphere," *Geophys. J. Int.*, vol. 162, no. 3, pp. 655–675, May 2005.
[16] M. A. Wieczorek and F. J. Simons, "Minimum variance multitaper spectral estimation on the sphere," *J. Fourier Anal. Appl.*, vol. 13, no. 6, pp. 665–692, 2007.
[17] J. J. Sakurai, *Modern Quantum Mechanics*, 2nd ed. Reading, MA: Addison Wesley Publishing Company, Inc., 1994.
[18] J. McEwen and Y. Wiaux, "A novel sampling theorem on the sphere," *IEEE Trans. Signal Process.*, vol. 59, no. 12, pp. 5876–5887, Dec. 2011.
[19] T. Bülow, "Spherical diffusion for 3D surface smoothing," *IEEE Trans. Pattern Anal. Mach. Intell.*, vol. 26, no. 12, pp. 1650–1654, Dec. 2004.
[20] F. J. Narcowich and J. D. Ward, "Nonstationary wavelets on the m-sphere for scattered data," *Appl. Comput. Harmon. Anal.*, vol. 3, no. 4, pp. 324–336, Oct. 1996.
[21] J.-P. Antoine and P. Vandergheynst, "Wavelets on the 2-sphere: A group-theoretical approach," *Appl. Comput. Harmon. Anal.*, vol. 7, no. 3, pp. 262–291, 1999.
[22] Y. Wiaux, J. D. McEwen, P. Vandergheynst, and O. Blanc, "Exact reconstruction with directional wavelets on the sphere," *Mon. Not. R. Astron. Soc.*, vol. 388, no. 2, pp. 770–788, 2008.
[23] D. Marinucci, D. Pietrobon, A. Balbi, P. Baldi, P. Cabella, G. Kerkyacharian, P. Natoli, D. Picard, and N. Vittorio, "Spherical needlets for cosmic microwave background data analysis," *Mon. Rot. R. Astron. Soc.*, vol. 383, no. 2, pp. 539–545, 2008.
[24] J.-L. Starck, Y. Moudden, P. Abrial, and M. Nguyen, "Wavelets, ridgelets and curvelets on the sphere," *Astron. and Astrophy.*, vol. 446, no. 3, pp. 1191–1204, Feb. 2006.
[25] G. Boudreaux-Bartels and T. Parks, "Time-varying filtering and signal estimation using Wigner distribution synthesis techniques," *IEEE Trans. Acoust., Speech, Signal Process.*, vol. 34, no. 3, pp. 442–451, Jun. 1986.
[26] B. E. A. Saleh and N. S. Subotik, "Time-variant filtering of signals in the mixed time-frequency domain," *IEEE Trans. Acoust., Speech, Signal Process.*, vol. 33, no. 6, pp. 1479–1485, Dec. 1985.
[27] L. Cohen, "Time frequency filtering," in *Proc. IEEE Int. Conf. Acoust., Speech, Signal Process. (ICASSP)*, Apr. 1988, pp. 2212–2215.

[28] F. Hlawatsch, W. Kozek, and W. Krattenthaler, “Time-frequency subspaces and their application to time-varying filtering,” in *Proc. IEEE Int. Conf. Acoust., Speech, Signal Process. (ICASSP)*, Apr. 1990, vol. 3, pp. 1607–1610.

[29] W. Kozek and F. Hlawatsch, “A comparative study of linear and nonlinear time-frequency filters,” in *Proc. IEEE-SP Int. Symp. Time-Freq., Time-Scale Anal., 1992*, Oct. 1992, pp. 163–166.

[30] L. Cohen, *Time-Frequency Analysis: Theory and Applications*. Englewood Cliffs, NJ: Prentice-Hall, Inc., 1995.

[31] R. L. Allen and D. W. Mills, *Signal Analysis: Time, Frequency, Scale and Structure*. Piscataway, NJ: IEEE Press, 2004.

[32] B. Boashash, *Time Frequency Signal Analysis and Processing: A Comprehensive Reference*. , UK: Elsevier, 2003.

[33] M. L. Kramer and D. L. Jones, “Improved time-frequency filtering using an STFT analysis-modification-synthesis method,” in *Proc. IEEE-SP Int. Symp. Time-Freq., Time-Scale Anal., 1994*, Oct. 1994, pp. 264–267.

[34] M. Simons, S. C. Solomon, and B. H. Hager, “Localization of gravity and topography: Constraints on the tectonics and mantle dynamics of venus,” *Geophys. J. Int.*, vol. 131, no. 1, pp. 24–44, Oct. 1997.

[35] Z. Khalid, S. Durrani, P. Sadeghi, and R. A. Kennedy, “Spatio-spectral analysis on the sphere using spatially localized spherical harmonics transform,” *IEEE Trans. Signal Process.*, vol. 60, no. 3, pp. 1487–1492, Mar. 2012.

[36] T. Risbo, “Fourier transform summation of Legendre series and D-functions,” *J. Geodesy*, vol. 70, pp. 383–396, 1996.

[37] B. D. Wandelt and K. M. Górski, “Fast convolution on the sphere,” *Phys. Rev. D*, vol. 63, no. 12, p. 123002, May 2001.

[38] F. J. Simons, J. C. Hawthorne, and C. D. Beggan, “Efficient analysis and representation of geophysical processes using localized spherical basis functions,” in *Wavelets XIII*. Bellingham, WA: SPIE, 2009, vol. 7446, p. 74460G.

[39] A. Albertella, F. Sansò, and N. Sneeuw, “Band-limited functions on a bounded spherical domain: The Slepian problem on the sphere,” *J. Geodesy*, vol. 73, no. 9, pp. 436–447, Jun. 1999.

[40] W. Freeden and V. Michel, “Constructive approximation and numerical methods in geodetic research today – An attempt at a categorization based on an uncertainty principle,” *J. Geodesy*, vol. 73, no. 9, pp. 452–465, 1999.

[41] L. Cohen, “Time-frequency distributions—A review,” *Proc. IEEE*, vol. 77, no. 7, pp. 941–981, Jul. 1989.

[42] W. Krattenthaler and F. Hlawatsch, “Time-frequency design and processing of signals via smoothed Wigner distributions,” *IEEE Trans. Signal Process.*, vol. 41, no. 1, pp. 278–287, Jan. 1993.

[43] D. W. Jepsen, E. F. Haugh, and J. O. Hirschfelder, “The integral of the associated Legendre function,” *Proc. Nat. Acad. Sci. USA.*, vol. 41, no. 9, pp. 645–647, Sep. 1955.

[44] L. C. Biedenharn and J. D. Louck, *Angular Momentum in Quantum Physics: Theory and Application*. Reading, MA: Addison Wesley, 1981.

[45] F. Dahlen and F. J. Simons, “Spectral estimation on a sphere in geophysics and cosmology,” *Geophys. J. Int.*, vol. 174, pp. 774–807, 2008.

Zubair Khalid (S’10) received the B.Sc. (first-class hons.) degree in electrical engineering from the University of Engineering & Technology (UET), Lahore, Pakistan, in 2008. He is currently working toward the Ph.D. degree from the Research School of Engineering, the Australian National University, Canberra, Australia.

Zubair was awarded University Gold Medal and Industry Gold Medals from Siemens and Nespak for his overall outstanding performance in Electrical Engineering during the his undergraduate studies. He is a recipient of an Endeavour International Postgraduate Award for the duration of his Ph.D. He was also awarded an ANU Vice Chancellor’s Higher Degree Research (HDR) travel grant in 2011. His research interests are in the area of development of novel signal processing techniques for signals on the sphere.

Parastoo Sadeghi (S’02–M’06–SM’07) received the B.E. and M.E. degrees in electrical engineering from Sharif University of Technology, Tehran, Iran, in 1995 and 1997, respectively, and the Ph.D. degree in electrical engineering from The University of New South Wales, Sydney, Australia, in 2006.

From 1997 to 2002, she worked as a Research Engineer and then as a Senior Research Engineer at Iran Communication Industries (ICI) in Tehran, Iran and at Deqx (formerly known as Clarity Eq) in Sydney, Australia. She is currently a Fellow at the Research School of Engineering, The Australian National University, Canberra, Australia. She has visited various research institutes, including the Institute for Communications Engineering, Technical University of Munich, from April to June 2008, and MIT from February to May 2009. She has coauthored more than 80 refereed journal or conference papers and is a Chief Investigator in a number of Australian Research Council Discovery and Linkage Projects. Her research interests are mainly in the area of wireless communications systems and signal processing.

Dr. Sadeghi received two IEEE Region 10 Student Paper Awards for her research in the information theory of time-varying fading channels, in 2003 and 2005.

Rodney A. Kennedy (S’86–M’88–SM’01–F’05) received the B.E. degree from the University of New South Wales, Sydney, Australia, in 1982, the M.E. degree from the University of Newcastle, in 1985, and the Ph.D. degree from the Australian National University, Canberra, in 1988.

He is currently a Professor in the Research School of Engineering, Australian National University.. His research interests include digital signal processing, digital and wireless communications, and acoustical signal processing.

Salman Durrani (S’00–M’05–SM’10) received the B.Sc. (1st class hons.) degree in electrical engineering from the University of Engineering and Technology, Lahore, Pakistan, in 2000. He received the Ph.D. degree in electrical engineering from the University of Queensland, Brisbane, Australia, in 2004.

He has been with the Australian National University, Canberra, Australia, since 2005, where he is currently a Senior Lecturer in the Research School of Engineering, College of Engineering and Computer Science. He serves as a Technical Program Committee Member for international conferences such as ICC ’13, PIMRC ’12 and AusCTW ’12. His current research interests are in wireless communications and signal processing, including synchronization in cooperative communication systems, connectivity of ad-hoc networks and vehicular networks and signal processing on the unit sphere. He has 55 publications to date in refereed international journals and conferences.

Dr. Durrani was awarded an ANU Vice-Chancellor’s Award for Teaching Excellence in 2012. He was a recipient of an International Postgraduate Research Scholarship from the Australian Commonwealth during 2001–2004. He was awarded a University Gold Medal during his undergraduate studies. He is a Member of Institution of Engineers, Australia.